Journal Of Hazardous Materials
April 2023, Volume 448 Pages 130858 (13p.)
https://doi.org/10.1016/j.jhazmat.2023.130858
https://archimer.ifremer.fr/doc/00818/92995/

Keystone microbial taxa organize micropollutant-related modules shaping the microbial community structure in estuarine sediments

Veloso Sandrine [1], Amouroux David [1], Lanceleur Laurent [2], Cagnon Christine [1], Monperrus Mathilde [2], Deborde Jonathan [2, 3], Laureau Cristiana Cravo [1], Duran Robert [1, *]

[1] Universite de Pau et des Pays de l'Adour, E2S UPPA, CNRS, IPREM, Institut des Sciences Analytiques et de Physico-chimie pour l'Environnement et les matériaux, Pau, France
[2] Universite de Pau et des Pays de l'Adour, E2S UPPA, CNRS IPREM, Institut des Sciences Analytiques et de Physico-chimie pour l'Environnement et les matériaux, Anglet, France
[3] Ifremer, LITTORAL, Laboratoire Environnement Ressources des Pertuis Charentais, F-17390 La Tremblade, France

* Corresponding author : Robert Duran, email address : robert.duran@univ-pau.fr

Abstract :

The fluctuation of environmental conditions drives the structure of microbial communities in estuaries, highly dynamic ecosystems. Microorganisms inhabiting estuarine sediments play a key role in ecosystem functioning. They are well adapted to the changing conditions, also threatened by the presence of pollutants. In order to determine the environmental characteristics driving the organization of the microbial assemblages, we conducted a seasonal survey along the Adour Estuary (Bay of Biscay, France) using 16S rRNA gene Illumina sequencing. Microbial diversity data were combined with a set of chemical analyses targeting metals and pharmaceuticals. Microbial communities were largely dominated by Proteobacteria (41 %) and Bacteroidota (32 %), showing a strong organization according to season, with an important shift in winter. The composition of microbial communities showed spatial distribution according to three main areas (upstream, middle, and downstream estuary) revealing the influence of the Adour River. Further analyses indicated that the microbial community was influenced by biogeochemical parameters (Corg/Norg and 13C) and micropollutants, including metals (As, Cu, Mn, Sn, Ti, and Zn) and pharmaceuticals (norfloxacin, oxolinic acid and trimethoprim). Network analysis revealed specific modules, organized around keystone taxa, linked to a pollutant type, providing information of paramount importance to understand the microbial ecology in estuarine ecosystems.

Graphical abstract

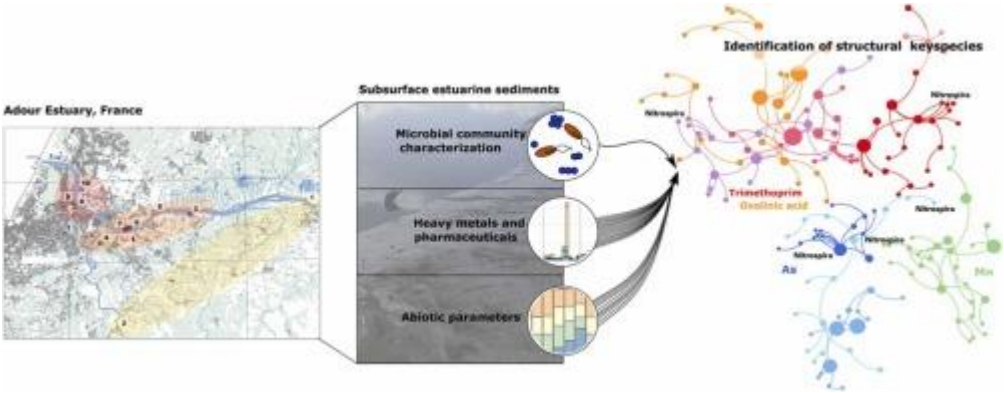

Highlights

► Contamination hot spots were identified in urban area of the Adour Estuary. ► The abundance of specific taxa was correlated with micropollutant concentrations. ► Keystone taxa drive microbial networks according to micropollutant contents. ► *Nitrospira,* keystone taxa in various conditions, might represents an ideal partner.

Keywords : Multi-contamination, Sequencing, Co-occurrence network, Microbial ecology, Antibiotics

Environmental implication

The study aims to decipher the impact of anthropogenic multi-contamination on microbial communities in the Adour Estuary (France) sediments in order to identify the main environmental drivers as well as the keystone microbial taxa organizing the microbial communities.

The environmental conditions (hydrological and geochemical parameters; metals and pharmaceuticals content) combined with 16S rRNA gene metabarcoding data, revealed the effect of antibiotics and metals contamination on microbial community structures. We propose that *Nitrospira*, identified as keystone microbial taxa establishing microbial relationships under various contamination levels, corresponds to an ideal partner that should be considered when implementing strategies for environmental management.

1 Introduction

Estuaries are ecotones, transitional waters at the interface of freshwater and marine habitats. They are described as highly productive areas providing ecosystem services such as nurseries for many bird and fish species, regulation of nutrient flow and cycling, and recreational activities (Kennish, 2002; Basset et al., 2013). They are highly sensitive environments showing important fluctuations of environmental parameters, including salinity, temperature, and nutrient concentrations. Estuaries have been considered as naturally stressed environments (Elliott and Quintino, 2007), further threatened by various contaminants released by human activities. Among the contaminants, metals and pharmaceuticals are of primary concern because they are biologically active compounds threatening aquatic biota, ecosystems and even human health (Fabbri and Franzellitti, 2016). These compounds are ubiquitous, being detected in various estuarine compartments, including surface water (Aminot et al., 2016; Obimakinde et al., 2017), effluent from wastewater treatment plants (Li et al., 2016), sediments (Shi et al., 2014), and aquatic organisms (He et al., 2019). Microorganisms play a crucial role in numerous environmental processes and functions, being involved in carbon, nitrogen, phosphorus cycles (Bauer et al., 2013; Damashek and Francis, 2018; Watson et al., 2018). In estuarine sediments, microorganisms are highly diverse with complex organization, representing the main biotic compartment (Lozupone and Knight, 2007; Yi et al., 2020). The microbial communities are sensitive to environmental variations such as temperature and salinity, and the presence of micropollutants (Lozupone and Knight, 2007; Sun et al., 2012; Jeanbille et al., 2016). Hence, in ecosystems as much fluctuating than estuaries, the shift in microbial community structuration are likely to be observed in response to the input of metals and pharmaceuticals. The presence of pollutants, both organic and inorganic, has been shown to influence the organization of microbial communities in aquatic environments (Bordenave et al., 2004; Vercraene-Eairmal et al., 2010; Cravo-Laureau et al., 2011; Duran et al., 2015). It is thus of paramount importance to understand how micropollutants in sediment modify the microbial community structure in order to identify key microorganisms around which microbial assemblages are organized in response to the presence of a pollutant. Network analysis allows to determine the interactions between microorganisms and other organisms and their habitat (Fuhrman and Steele, 2008; Williams et al., 2014),

revealing ‘specialists’ microorganisms specifically associated with a pollutant type and its biotic interactions (Lladó et al., 2015; Duran et al., 2015).

The Adour Estuary (France), located in the Bay of Biscay (Atlantic Ocean), features contrasted areas that are under the influence of different human activities, exhibiting different types and levels of pollution (Stoichev et al., 2004). The upstream of the watershed is mainly agricultural with livestock activities, while downstream is highly urbanized, with industrial, port and urban activities.

In this work, we hypothesize that the environmental factors influence the organization of microbial assemblage in sediments. Particularly, the presence of pollutants promotes the selection of specific taxa that represent potential biomarkers of pollution, although estuarine environments constitute highly mixing zones. The main objective of the study was thus to characterize the relationships between the microbial communities, hydrological and geochemical characteristics, and pollutants occurrence and content (metals and pharmaceuticals), in estuarine sediments along ten sampling sites located in the Adour Estuary at different seasons, in order to estimate the significant parameters driving the estuarine microbial communities.

2 Material and Methods

2.1 Study site and sample collection

The Adour Estuary is located at the southwestern of France, extends along 308 km from the Pyrenees to the Bay of Biscay (Atlantic North-East). This mesotidal estuary presents a highly heterogenous content river discharge, with 290 $m^3.s^{-1}$ in annual mean and varying between 50 and 3,200 $m^3.s^{-1}$. Three sampling campaigns were performed: May 2017 (spring), September 2017 (summer), and from January to February 2018 (winter). Samples were collected at low tide slackwater, the tidal coefficient ranged between 78 and 109. Estuarine sediments were sampled in ten sites from maximum salinity intrusion in the Adour River (site 1) and in the Nive River (site 2) to the downstream estuary (site 10) (Fig. 1). Sites were selected in order to sample both upstream preserved sites and downstream contaminated sites according to area structuration and previous observations (Stoichev et al., 2004; Point, 2004; Cavalheiro et al., 2017). Triplicate of surface sediment samples (0 - 1 cm) were collected in sealable plastics bags. In total, the analyses

were performed on 90 samples (10 sites * 3 replicates * 3 seasons). Samples were transported in coolers at approximately 4°C and in the dark to the laboratory, within 2h. Samples were then stored at -20°C until analysis. During sample collection, an aliquot of each replicate was stored specifically in 2 mL Eppendorf tubes directly shock-frozen in liquid nitrogen carriers and stored at −80°C prior microbial DNA extraction.

2.2 Hydrological and geochemical characteristics

Sediments were freeze-dryed in a freeze-dryer (VaCo2 - Zirbus, Germany). Dry sediments were visually homogenized, plants, stone and other debris were manually removed. An aliquot of 1 g was collected for grain size distribution characterization by laser diffraction (Mastersizer 2000, Malvern). Sediments were then grinded in a planetary ball mill (PM 100, Retsch) and stored at -20°C. Sediments water contents (%WC) were obtained by measuring the weight loss before and after drying at 60°C for 48h. Total carbon and particulate organic carbon (TC and POC) were analyzed by infrared spectroscopy via high temperature combustion on a Shimadzu TOC-LCSH/CSN/SSM-5000A analyzer. POC was measured after removal of carbonates with 1.2 N HCl from 200 mg of powdered sample. Sediments for carbon and nitrogen isotopic compositions, particulate organic nitrogen (PON) and C/N ratios were weighed into silver cups and decarbonated using 1.2 N HCl, and then analyzed using an elemental analyzer (Flash 2000, Thermo Fisher Scientific) coupled to an isotope ratio mass spectrometer (IRMS; Isoprime, GV Instruments). Chlorophyll-*a* was measured in sediments by spetrophotometry according to Lorenzen (1967) and Aminot and Kérouel (2004) using a Shimadzu UV-1800 spectrophotometer. All concentrations were expressed in dry weight. River discharge values were obtained from HYDRO database (http://hydro.eaufrance.fr).

2.3 Micropollutants characterization: Metals, trace elements and pharmaceuticals analyses

Trace metals and metalloids (Ag, As, Cd, Co, Cr, Cu, Mn, Mo, Ni, Pb, Sb, Se, Sn, Th, Ti, U, V, Zn) except Hg were measured in 0.05 to 1 g sample of dry sediments after an acid digestion and by inductively coupled plasma-mass spectrometry (ICP-MS; 7500 series, Agilent). Briefly, 3 mL of HNO_3 (70%, Instra Analysed, J.T. Baker) and 1 mL of HCl (37%, Ultrex, Fisher Scientific)

were added to dried sediment samples in acid-cleaned and uncolored PP tubes (DigiTUBE, SCP Science). Sediments solutions were heated on a hot plate at 85°C for 4h (DigiPREP, SCP Science). Then, 1 mL of hydrogen peroxide (30-32%, Optima, Fisher Chemical) was added drop by drop and solutions were heated again at 85°C for 2h (DigiPREP, SCP Science). Final volumes were adjusted to 15 mL with ultrapure water (MilliQ, Millipore). Solutions were centrifugated and the supernatants were filtered with 0.22 µm PTFE (Millipore) syringe filters. Filtrates were spiked with internal standards (Bismuth, Bi). Samples were analyzed by ICP-MS using the external calibration method with internal standard correction (Bi) and limits of detection are detailed in Table S1.

Quality of analyses was controlled with Standard Reference Materials (SRM 1944, National Institut of Standards & Technology), with mean recoveries ranging, with a few exceptions (2 out of 16), from 42 to 128%. Total mercury (Hg) content was measured by atomic absorption spectrophotometry (AAS) (Costley et al., 2000) using Advanced Mercury Analyzer (AMA-254, LECO). To avoid any grain size effect, trace metal concentrations were normalized with thorium (Th) concentrations (Lanceleur et al., 2011). For further analyses and statistics, triplicate samples were averaged per site.

A total of 43 pharmaceuticals was measured in surface sediment by liquid chromatography coupled to tandem mass spectrometry (LC- MS/MS), including 7 non-steroidal anti-inflammatory drugs (acetaminophen, aspirin, niflumic acid, diclofenac, ibuprofen, ketoprofen and phenazone), 22 antibiotics (ampicillin, azithromycin, ciprofloxacin, clarithromycin, doxycycline, erythromycin, flumequine, josamycin, metronidazole, norfloxacin, ofloxacin, oxolinic acid, piperacillin, rifampicin, roxithromycin, spiramycin, sulfadiazine, sulfamethazine, sulfamethoxazole, tetracycline, trimethoprim and tylosin), 3 anxiolytics (lorazepam, nordazepam and oxazepam), 3 cardiovascular drugs (atenolol, losartan and metoprolol), as well as an antiarrhythmic agent (amiodarone), an anticancer drug (cyclophosphamide), one hormone (norethindrone), a diuretic (hydrochlorothiazide), a compound from fibrate group of medications (gemfibrozil), a diuretic and carbonic anhydrase inhibitor (acetazolamide), a neuroleptic (carbamazepine) and caffeine. The latter can be considered as a stimulant and can be used as a domestic sewage tracer since it is one of the most consumed substances worldwide (Quadra et al., 2020). Internal standard solutions were composed of carbamazepine-d10, atenolol-d7,

ciprofloxacin-d8, norfloxacin-d5, ofloxacin-d3, diazepam-d5, nordazepam-d5 and ibuprofen-d3. All internal standards were purchased from Sigma-Aldrich. Extraction of pharmaceuticals in surface sediment was performed following the micro-QuEChERS (Quick, Easy, Cheap, Effective, Rugged and Safe) method coupling solid extraction protocol (Ben Salem et al. 2016; Siedlewicz et al. 2016; Azaroff, et al. 2020) and liquid SPE pre-concentration protocol (Gros et al. 2017). As previously described, the sample volume was adapted to reduce the matrix effect (Maillet et al. 2017; Guironnet et al. 2022) optimizing the recovery of important sensitive pharmaceuticals (Peysson and Vulliet, 2013). Briefly, extraction was processed by adding to 200 mg of dry sediment spiked with 40 µL of internal standard solutions (at 50 $mg.L^{-1}$ in methanol), a mixture of 1 mL methanol (MeOH), 1 mL supersaturated aqueous ammonium chloride solution and 200 µL Na_2EDTA at 0.1 $mol.L^{-1}$ (Sigma Alrich). Samples were sonicated for 8 min and centrifuged 5 min at 4,500 rpm. Supernatant were collected and transferred into 50 mL polypropylene tubes. Sample volume was adjusted to 50 mL with ultrapure water (MilliQ, Millipore). Solutions were loaded in Oasis HLB cartridges (60 mg, 3 cc) (Waters) previously conditioned with 3 mL MeOH followed by 3 mL MeOH at 1 $mL.min^{-1}$. After loading samples, cartridges were rinced with 5 mL ultrapure water and dried at room temperature for 20 min. Elution solvent was 5 mL MeOH at flow rate 1 $mL.min^{-1}$. Samples were evaporated under a gentle air stream (TurboVap LV, Biotage). Dried extracts were then reconstituted in 1 mL MeOH:H_2O (MilliQ) (5: 95, v:v) and stored at -20°C prior to analysis by LC-MS/MS using an Acquity UPLC system connected to a Xevo TQ MS (Triple quadru- pole) with an electrospray (ESI) interface (Waters). An internal calibration with deuterated analogs was used to quantify concentrations of target compounds. Two matrix-matched calibration curves were prepared using 200 mg of sediments with different granulometry (sandy and silty) spiked with increasing concentration of target pharmaceuticals ranging from 0 to 500 $ng.g^{-1}$. Solvent blanks (MeOH:H_2O, 5: 95, v:v) and procedural blanks were prepared to evaluate system performances and detection limits (Table S1). Recoveries were measured from sediment samples adding a mixture of selected pharmaceuticals at the concentration of 200 $ng.g^{-1}$. With a few exceptions (6 out of 44 compounds), recoveries ranged between 80 and 110%.

2.4 Microbial community composition

Total DNA was extracted from environmental samples (~500 mg of wet sediment) using PowerSoil DNeasy (Qiagen) according to the manufacturer's instructions. The microbial universal primers 515F-Y 5'-GTGYCAGCMGCCGCGGTAA-3' (Parada et al., 2016) and 926R 5'-CCGYCAATTYMTTTRAGTTT-3' (Quince et al., 2011) were used to amplified V4-V5 hypervariable 16S rRNA gene regions. Triplicate polymerase chain reaction (PCR) reaction mixtures containing 1 µL of DNA at 10 ng.µL^{-1}, 2X AmpliTaq Gold DNA Polymerases (Thermo Fisher Scientific), 0.5 µM forward primer, 0.5 µM indexed reverse primer in a final reaction volume of 25 µL. PCR amplification conditions were an initial denaturing step of 10 min at 95°C followed by 35 cycles of 95°C for 30 s, 60°C for 30 s and 72°C for 45 s and then a final extantion of 7 min at 72°C. Per sample, a pool of triplicate PCR reaction was sent to Genotoul (INRA Toulouse, France) for sequencing process. Amplicon were sequenced using MiSeq Illumina 2x 250 bp. Sequences were processed in R software (version 4.0.2) (R Core Team, 2020). R package dada2 (version 1.16.0) was used to analyze and cleaned 16S rRNA gene sequence reads and identified amplicon sequence variants (ASVs) (Callahan et al., 2016a) according to the default settings. The ASV identification was done using pseudo-pooling sample strategy. The taxonomic assignment of ASVs was made using SILVA SSU (small subunit) database (version 138) (Quast et al., 2013) and IDTAXA (Murali et al., 2018). The treatment of ASV and taxonomic table were processed with R package phyloseq (version 1.32.0) following instruction from Callahan et al. (2016b) but also including a rarefaction step (calculated on observed richness, R). After diversity analysis, within ASV and taxonomic table, replicates were merged by mean by site.

2.5 Statistical analysis

All graphics and statistical analyses were processed using R software (R Core Team, 2020). All analyses were performed on thorium-normalized data and average triplicates for chemical data. For sequencing data, the mean of triplicate for each sample was used to build the ASV table.

Principal component analysis (PCA) and non-metric multidimensional scaling (NMDS) were performed using vegan package (Oksanen et al., 2020) based on Bray-Curtis dissimilarity. Analysis of similarity (ANOSIM) were performed based on 999 permutation using vegan package. Permutational multivariate analysis of variance (PERMANOVA) based on 1,000

permutations using Bray-Curtis matrices and vegan R package were used to estimate the relative contribution of environmental variables. Canonical-correlation analysis (CCA) with 9,999 Monte Carlo permutation tests were conducted, with variables that present significant contribution on the PERMANOVA and ASV table at the genus taxonomic level, using vegan package.

2.6 Co-occurrence networks construction

Co-occurrence network was built from overall ASV profil (all campaign, all site) merge by site, under Molecular Ecology Network Analyses pipeline (MENAp) using a random matrix theory (RMT) based method (Zhou et al., 2011; Deng et al., 2012). Based on the relative proportion of ASVs abundance and ASVs present in a minimum of 37% of all samples (all campaigns included), networks were constructed using Pearson correlation matrix (Zhou et al., 2011). Within networks, modules, groups of nodes showing higher densities connections within each group than between (Newman, 2004), were identified by fast greedy modularity optimization (Newman, 2004; Clauset et al., 2004). Modules composed of a minimum of 5 nodes were conserved in further analysis. Gephi 0.9.2 was used to visualize resulting networks and modules (Bastian et al., 2009).

3 Results and discussion

3.1 Geochemical parameters and contamination level

Although the sites on the Adour Estuary were located in different areas, i) downstream and middle-stream estuarine area under urban contributions and ii) upstream area under agricultural and fluvial influence (Fig. 1), surface sediments exhibited homogenous geochemical patterns (Table S2). According to the isotopic signatures and C/N ratios, sediments were dominated by river derived organic matter with a slight proportion of organic matter from sewage treatment plants for urban sites (Savoye et al., 2012; Kubo and Kanda, 2017). These geochemical parameters did not show significant seasonal variations, but the chlorophyll-a and POC contents were higher in spring and summer, especially in downstream sites, suggesting that a major amount of sediment organic matter in the Adour Estuary came from autochthonous primary production (Kubo and Kanda, 2017).

The PCA, explaining 46% of the variance on the first two axes, showed that the samples were distinguished mainly by hotspots values (Fig. 2). The third axis of the PCA, explaining additional 11% of the variance, was also driven by the same hotspot values (Fig. S1). Nevertheless, the separation of samples according to location can be mainly observed along the axis 2, while the axes 1 and 3 discerned the samples mainly according to the season (Fig. 2, Fig. S1). The PCA showed the main distribution of samples as follows: i) the middle-stream sites were linked to metoprolol and abiotic parameters (water content and fraction < 50 μm), and Mn in winter and summer, ii) the upstream sites were linked to norfloxacin in summer and in winter, and Mo in spring, and iii) the downstream sites were associated to norethindrone, As and Sb in summer, to oxolinic acid in winter, and to Mo and Zn in spring (Fig. 2). However, the seasonal variability of both hydrological and geochemical parameters was not significant contrary to that observed in previous studies on the Adour Estuary (Stoichev et al., 2004), and even other estuaries (Shi et al., 2014; Aminot et al., 2016). The highest concentration of antibiotics was found in winter (Table S3), which corresponds to the highest Adour River discharge season contrarily to that observed in other estuaries (Liu and Wong, 2013; Aminot et al., 2016). The contamination profile of the Adour Estuary was characterized by higher contaminant concentrations in the middle (mainly site 7) or downstream estuarine Urban area (sites 8, 9 and 10), than upstream area (Fig. 2; Tables S3 to S6). Since it has been shown that the presence of contaminants plays a crucial role in shaping the structure of microbial communities (Misson et al., 2016; Jacquiod et al., 2018; Wang et al., 2021), the microbial communities were characterized in order to decipher the environmental parameters controlling the microbial assemblages.

3.2 Microbial community diversity and composition

The composition of microbial communities, determined by 16S rRNA sequencing, provided 16,288 ASVs (Amplicon Sequences Variants) coming from 1,629,171 reads (after filtration and chimera removal). A mean of 1,819 ASVs ± 494 (richness, R) per sample was obtained, which was consistent with previous reports showing similar diversity in estuarine sediments (Yan et al., 2018). Observed richness rarefaction curves showed a plateau (Fig. S2), suggesting that the sequencing effort was sufficient to collect most of the diversity. The microbial α-diversity

(Simpson evenness) was homogenous among samples (Table S7), indicating that the microbial diversity level was not affected by the presence of contaminants. It was surprising to observe such similar diversity indexes in sediments presenting different contaminant types and contents since previous studies showed that the presence of pollutants affects (increase or decrease) the microbial diversity (Johnston and Roberts, 2009; Duran et al., 2015; Jacquiod et al., 2018; Li et al., 2020). However, similar observations have been reported when comparing contaminated and non-contaminated sediments (Paissé et al., 2008; Ben Salem et al., 2019). The legacy of microbial communities exposed to fluctuating presence of contaminants combined with the coalescence of microbial communities, mixing microbial communities along tidal estuarine continuum, may explain the homogenous microbial diversity observed in the Adour Estuary. This was also previously proposed in river sediments (Yin et al., 2015).

After rarefaction step, in total 42 phyla were observed in this study. More than 80% of the relative abundance corresponded to two phyla: *Proteobacteria* (41 ± 3%) and *Bacteroidota* (32 ± 6%) (mean ± SD of all samples) (Fig. 3). The dominance of these two phyla is consistent with the major groups found in estuarine environments (Fortunato and Crump, 2015; Guo et al., 2018; Vidal-Durà et al., 2018), where they play a critical role in biogeochemical cycles (Xia et al., 2013). *Proteobacteria* were dominated by *Gammaproteobacteria* (23 ± 9%) and *Alphaproteobacteria* (9 ± 3%). The *Burkholderiales* order, formerly affiliated to *Betaproteobacteria* class now affiliated to *Gammaproteobacteria*, dominated the *Gammaproteobacteria* (20 ± 6%). Interestingly, the abundances of *Alphaproteobacteria* and *Burkholderiales* showed significant seasonal variability (pairwise wilcox test, p-value < 0.05) with opposite trends. From summer/spring to winter, corresponding to the intrusion of freshwater in the estuary due to higher Adour River discharge in winter, the abundance of *Alphaproteobacteria* decreased (from 11 to 7%) while that of *Burkholderiales* increased (from 16 to 25%). It is likely that the variation of the abundance of these taxa was a consequence of the variation of the Adour River discharge (maximum in winter) and the intrusion of freshwater in the estuary. Accordingly, previous reports showed that *Burkholderiales* occur commonly in estuarine and freshwater ecosystems (Aylagas et al., 2017; Roberto et al., 2018) while *Alphaproteobacteria* have been identified as a major group in marine microbial communities (Pommier et al., 2007; Zinger et al., 2011). The *Bacteroidetes* phylum, which members have been identified to play a crucial role in the degradation of biopolymers (e.g. chitin, cellulose)

(Fernández-Gómez et al., 2013; Kirchman, 2002), was dominated by the *Bacteroidia* class (30 ± 6%), especially by the *Flavobacteriales* order (Table S8). In accordance with previous report showing the critical role of the *Flavobacterium* genus in the microbial loop (detrital food web) (Kisand et al., 2002), the dominance of the *Flavobacterium* genus suggested that the organic matter played a key role in the organization of microbial communities in the Adour Estuary. Besides, several phyla were present in lower abundance in the bacterial community, including *Deltaproteobacteria* (*Desulfobacterota*; Waite et al., 2020), (5.5 ± 2.7%), *Acidobacteriota* (4.2 ± 2.2%), *Verrucomicrobiota* (3.1 ± 2.4%), *Actinobacteriota* (1.7 ± 0.9%), *Planctomycetota* (1.7 ± 0.8%), *Chloroflexi* (1.6 ± 0.8%), and *Firmicutes* (1.2 ± 0.9%). Members of these phyla are commonly found in estuarine or freshwater environments (Feng et al., 2009; Guo et al., 2018; Vidal-Durà et al., 2018). The *Archaea* were found at low abundance (< 1%) showing also seasonal variation, particularly in the estuarine Urban area, being not detected in spring while showing the highest abundance (1%) in winter. Despite such low abundance, it is worth to take into account *Archaea* since they are known to play an important role in biogeochemical cycles, especially the nitrogen cycle, methanogenesis and even metal resistance (Webster et al., 2015). The low abundance of *Archaea* in our study was in accordance with previous studies in similar ecosystems (Kaci et al., 2016; Vidal-Durà et al., 2018), although methodological bias underestimating Archaea, such as high variability of 16S rRNA gene for multiples *Archaea* lineages and a lack of specificity of universal primers for *Archaea* (Bahram et al., 2019), cannot be excluded. *Crenarchaeota*, *Halobacterota* and *Euryarchaeota*, were the main phyla, *Crenarchaeota* representing the more abundant archaeal phylum (> 0.2%; Fig. 3). These archaeal phyla are usually observed in estuarine sediment (Abreu et al., 2001; Kaci et al., 2016).

3.3 Spatial and seasonal variation in microbial community structure

ANOSIM showed that the microbial communities in the Adour sediment were grouped according to season ($R = 0.78$, p-value = 0.001), further confirmed by the hierarchical clustering (Fig. 4A) revealing that the microbial communities in winter were separated from those of the other seasons (ANOSIM, $R = 1$, p-value = 0.001). These results suggested that the microbial communities were influenced by seasonal parameters such as temperature and Adour River discharge (Table S2). Nevertheless, differences between microbial communities were also

observed along the Adour Estuary (ANOSIM, R = 0.15, p-value = 0.028), the NMDS analysis showing three clear clusters (Fig. 4B): microbial communities of upstream sites (1 and 2) being separated from those of the middle sites (3, 4, 5, 6 and 7) and downstream sites (8, 9 and 10). Noteworthy, the seasonal effect can be seen within these clusters in which the spring and summer microbial communities are clearly separated (Fig. 4A). Such observation was in accordance with the level of contaminant concentrations observed along the Adour Estuary showing a gradient of increasing pollutant concentration from upstream to downstream (Fig. 2; Tables S5 and S6), but the clear separation of the most upstream sites (1 and 2) from the other sites confirmed that they are under freshwater influence. It is likely that despite the microbial communities exhibited seasonal variations, they were adapted to both hydrological/geochemical conditions and contaminant concentrations prevailing at each site, as observed in other estuaries (Wang, L. et al., 2013; She et al., 2016; Guo et al., 2019).

3.4 Influence of micropollutants on microbial assemblages

3.4.1 Major parameters shaping microbial assemblages

Correlation and PERMANOVA analyses revealed that the microbial communities were influenced by 12 main environmental parameters (p-value < 0.05), including 6 metal(loid)s (As, Cu, Mn, Sn, Ti and Zn), 3 pharmaceuticals (norfloxacin, oxolinic acid and trimethoprim), C_{org}/N_{org}, $\delta^{13}C$, a parameter linked to organic matter transformation processes and the season (Table 1). Additional collinear parameters V, Co, losartan and flumequine respectively associated to As, Mn, Zn and oxolinic acid were also revealed (Table 1). Interestingly, the correlation of Zn, proxy used as urban water marker (Pringault et al., 2012), with losartan, antihypertensive drug, supported the urban contamination. However, oxolinic acid and flumequine, two quinolone antibiotics, are used in aquaculture and farming (cattle, pig and poultry) as well (Delépée et al., 2004). The presence of losartan together with Zn probably modifies the effect of Zn on microbial communities that has been shown to affect microbial activities (Pringault et al., 2008, 2010, 2012). The CCA also shows the link of Zn with pharmaceuticals, especially with the antibiotic norfloxacin (Fig. 5, Fig. S3). Interestingly, the CCA revealed that the abundance of 9 bacterial genera correlated with norfloxacin concentration (Fig. 5). Most of the genera are usually found in anaerobic digesters such as *Acetobacteroides*, *Acidaminobacter*, *Simplicispira*, *Leucobacter*,

Williamwhitmania, and *Comamonas* (Su et al., 2014; Wen et al., 2017; Szabó et al., 2017; Schumann and Pukall, 2017; Mei et al., 2020).

Additionally, the CCA showed the distribution of microbial communities according to their location in the estuary along the axis 2 (explaining 11% of the variation), while they were distributed according to the season mainly winter along the axis 1 (explaining 20% of the variation) and mainly spring along the axis 3 (explaining 8% of the variation; Fig. S3). The CCA showed that: i) the upstream sites were driven by trimethroprim in spring and summer, and oxolinic acid in winter, ii) the middle-stream sites were associated to the organic carbon/nitrogen ratio (C_{org}/N_{org}) in spring and summer, and to Cu and Ti in winter, and iii) the downstream sites were driven by As and Sn in spring and summer, and by Cu and Ti in winter (Fig. 2. Fig. S3). Farming activities, such as cattle, sheep, pig and poultry breeding and aquaculture, on the watersheds could be related with the exposure of microbial communities to antibiotics (trimethoprim and oxolinic acid) probably on upstream sites. Several bacterial genera were found associated with trimethoprim, including genera belonging to *Plantomycetes* (*Gemmata* and *Fimbriiglobus*) known to exhibit wide antibiotic resistance (Godinho et al., 2019).

Similarly, twelve genera were associated to oxolonic acid. The majority exhibit potential antibiotic resistance, including two members of *Chitinophagaceae* (*Terrimonas* and *Ferruginibacter*) (Cui et al., 2021), *Haliscomenobacter* (Zhang et al., 2020), *Geobacter* (Kashefi et al., 2003), *Deefgea* (Chen et al., 2010), JGI 0001001-H03 belonging to *Blastocatellaceae* (Jauregi et al., 2021) or again *Haliangium*, a genus known to synthetize antimicrobial compound (Sun et al., 2016). Moreover, the CCA showed the association of As and Sn with specific bacterial genera, including among them *Desulfosarcina, Defluviitaleaceae UCG-011, Propionigenium*, *Ruminococcus*, *Malonomonas*, *Macellibacteroides* described as anaerobic bacteria (Schink and Pfennig, 1982; Dehning and Schink, 1989; Jabari et al., 2012), together with the cyanobacteria *Chroococcidiopsis*, *Calothrix* (Boone and Castenholz, 2001) and other aerobic bacteria such as *Craurococcus*, *Imperialibacter*, *Rubellimicrobium* (Saitoh et al., 1998; Wang, H. et al., 2013; Jiang et al., 2019).

3.4.2 Microbial co-occurrence network description

The interactions between various microbial functional groups are pivotal for ensuring ecosystem functioning, as shown for fluctuating polluted environments (McGenity et al., 2012; Duran et al., 2015). In order to deeper describe the microbial relationships and their interactions with contaminants (metals and pharmaceuticals), a co-occurrence network was constructed based on strong and significant Spearman correlations. The microbial network contained 347 nodes and 404 edges, with topological features of complex systems such as scale-free, small-world, and modularity (M) (Table S9) indicating non-random network as previously proposed (Wan et al., 2020). The microbial network possessed high connectivity and modularity (Table S9) suggesting stability and resilience of the system as reported for microbial networks in paddy soil (Wan et al., 2020) and marine coastal sediment (Jeanbille et al., 2016). Following the 16S rRNA gene composition, the microbial network was dominated by *Proteobacteria* (40%), *Bacteroidetes* (25%), *Desulfobacterota* (7%), *Acidobacteriota* (6%), *Planctomycetota* (4%), and *Verrucomicrobiota* (4%) (Fig. 6A1).

Modularity analysis identified a total of 17 modules structuring the network, each composed of 9 to 29 nodes. Noteworthy, the modules were mainly composed by ASVs occurring in summer and/or spring (Fig. S6), probably because the ASV associated to winter did not show the minimal occurrence required for network construction (Liu et al., 2015), in accordance with the seasonal variability observed by CCA (Fig. 5). The modules correspond to groups of strongly connected ASVs within the group but with very few connections outside the group. Modules showing significant correlations (p-value < 0.05) with the most significant pollutants (PERMANOVA, Table 1) were detected (Fig. 6B).

Some modules showed negative correlations with environmental parameters (Fig. 6B) suggesting that these modules gathered microbial taxa either sensitive to metals (modules 4, 5, 6, 9, 12 and 15) or to antibiotics (modules 8 and 11). Such sensitive microbial taxa might be useful to report ecosystem quality, as for example in the MicrogAmbi integrative microbial community index combining sensitive and tolerant taxa (Aylagas et al., 2017). However, further investigations are required to understand the role of such sensitive microbial taxa in the ecosystem functioning. The other modules showed positive correlations with either antibiotics (modules 1, 6, 9, and 15) or metals (modules 8, 10, 11, and 16) (Fig. 6B). It was surprising that none of the modules correlate

with both antibiotics and metals since several studies have shown co-selection of resistances to these two kinds of compounds (Baker-Austin et al., 2006; Liu et al., 2021).

3.4.3 Antibiotics correlated modules

Regarding the modules positively correlated to antibiotics, four were correlated to both oxolinic acid and trimethoprim (modules 1, 6, 9, and 15), while the module 7 was correlated only with oxolinic acid (Fig. 6B). Both antibiotics, used in human and animal therapies, have been detected together in effluents of wastewater treatment plants (Rodriguez-Mozaz et al., 2020). The modules correlated with both trimethoprim and oxolinic acid (modules 1, 6, 9, and 15) were structured around ASVs affiliated to *Hydrogenophaga*, *Ignavibacterium*, *Leptospira* genera, and *Comamonadaceae* family, which represented keystone ASVs by exhibiting the highest connectivity within the network (Fig. 6C). The *Comamonadaceae* family, harboring a large diversity of metabolisms (Willems, 2014), to which *Hydrogenophaga* genus belongs. *Ignavibacterium album*, the unique member of *Ignavibacteriaceae* family, was isolated from microbial mats developed in hot spring water streams (Iino et al., 2010). Some species of *Leptospira* sp. are pathogen, responsible of leptospirosis, a disease targeting humans and animals (Costa et al., 2015). These three genera have been reported to show resistance to trimethoprim and/or oxolinic acid, as well as to other antibiotic (Chakraborty et al., 2010; Iino et al., 2010; Gerzova et al., 2014). In addition, the modules included several less connected ASVs, which related genera were reported as trimethoprim resistant, such as: *Geobacter* (modules 1 and 6) (Kashefi et al., 2003), *Gemmata* (module 1) (Cayrou et al., 2010), and *Pseudomonas* (module 15) (Meng et al., 2020) that is also known as oxolinic acid resistant (Concha et al., 2021). It is also worth to note that other genera, including *Luteolibacter* (module 1) (Pascual et al., 2017), *Nitrospira* (modules 1 and 9) (Mehrani et al., 2020), or *Terrimonas*, *Hyphomicrobium*, *Ferruginibacter* (module 9) (Cui et al., 2021) have been described as antibiotic-resistant taxa. The presence of well-structured microbial modules around antibiotic-resistant taxa represents an important concern for human health that should be considered in monitoring aquatic environment.

3.4.4 Metal(loid)s correlated modules

Regarding the modules positively correlated to metal(loid)s (Fig. 6B), one was correlated to Mn (module 10) and three to As (modules 8, 11, and 16). The concentration of these elements ranged between 176 and 1,100 $\mu g.g^{-1}$ for Mn and 6.6 and 19 $\mu g.g^{-1}$ for As (Tables S4 and S6). These concentrations are between the lowest effect level (LEL; 460 and 6 $\mu g.g^{-1}$ for Mn and As respectively) and the severe effect level (SEL; 1100 $\mu g.g^{-1}$ and 33 $\mu g.g^{-1}$ for Mn and As respectively) for sediment (Persuad et al., 1993), indicating that Mn and As can reach a moderate contamination level in the Adour Estuary.

The module 10, significantly correlated to Mn, included keystone ASVs affiliated to *Lewinella*, uncultured IheB3-7 bacteria, and two ASVs corresponding to the families of *Comamonadaceae* and *Rhodobacteraceae* (Fig. 6C2). *Lewinella* and the uncultured IheB3-7 bacteria are marine bacteria, typically found in sediment and deep-sea systems respectively (Nakagawa et al., 2005). Interestingly, several members of *Comamonadaceae* family are recognized as manganese-oxidizing bacteria (Breda et al., 2017). Mn-oxides have been shown to be involved in the nitrogen cycle, Mn geochemistry being important for controlling redox processes in sediments (Anschutz et al., 2019). Beside these keystone ASVs, the module gathered several ASVs that have been described for their Mn removal capacity such as ASVs associated to the *Flavobacteriaceae* and *Pirellulaceae* families (Carmichael et al., 2013; Molari et al., 2020), *Nitropira* and *Oscillatoria* genera (Gerasimenko et al., 2013; Palomo et al., 2016) as well as metal(loid)s resistant genera such as *Arenimonas* and *Roseomonas* (Li, F. et al., 2021; Wang, F. et al., 2021).

The modules correlated to As were organized around keystone ASVs affiliated to *Rhodobacteraceae* and *Holophagaceae* (module 8), *Ekhidna*, *Pir4 lineage* and TRA3-20 family (module 11) and *Nitrospira* (module 16) (Fig. 6C3). Some of the genera have been described as As resistant taxa, including the genera of the *Rhodobacteraceae* (Crognale et al., 2019) and *Holophagaceae* (Islam et al., 2005; Stroud et al., 2014) families, and members of the *Nitrospira* genera (Palomo et al., 2018). Such observations supported their structuring role in As resistant modules. It was particularly interesting to found *Nitrospira*, a nitrite-oxidizing genera able to perform complete nitrification (comammox), which has been demonstrated to carry As resistance mechanisms (Palomo et al., 2018). *Nitrospira* might play a crucial role promoting the formation

of bacterial assemblages in association with other ASVs related to *Dechloromonas* (module 8) and *Aquabacterium* (module 16) As resistant genera (Suhadolnik et al., 2017). Additionally, the modules correlated with As included sulphate-reducing bacteria (SRB) *Desulfonatronobacter*, *Desulfuromonadia* (module 16), and *Desulfobulbus* (module 8), which have been shown involved in As methylation and demethylation processes (Chen et al., 2019). Such observation is in accordance with several studies reporting the presence of SRB and other sulphate-reducing microorganisms (SRM) in As rich environments (Dias et al., 2008; Bruneel et al., 2008; Giloteaux et al., 2013; Liu et al., 2018). SRM might play a crucial role in the organization of microbial networks in response to As.

The presence of ASVs related to *Nitrospira* in almost all modules significantly correlated with pollutants was the most striking observation, which suggested that the presence of *Nitrospira* is an essential link in the microbial networks. Such omnipresence of *Nitrospira* is probably explained by its involvement on the nitrogen cycle, particularly via comammox, combined with its capacity to face the presence of organic and inorganic contaminants (Palomo et al., 2018). The presence of *Nitrospira* has been reported in microbial networks in various ecosystems, including wastewater treatment plant (Petrovski et al., 2020), saline soil (Li, X. et al., 2021), alpine grassland (Qi et al., 2021), agricultural soil (Han et al., 2021), estuarine mudflat (Wang, X. et al., 2021). Such cosmopolitan behaviour suggests that *Nitrospira* is a “good friend”, an ideal partner for microorganisms for the colonization of a wide range of habitats. Such capability is particularly interesting for treatments of contaminated sediments, making *Nitrospira* a potential bio-augmentation agent.

4 Conclusion

Our study shows the stratification of microbial communities along an estuarine continuum highlighting the fragmentation according to habitat filtering despite the mixing zone that represents the conditions conductive to the coalescence of microbial communities. Specific microbial communities were observed, depending on the occurrence and level of contaminants, that allowed to detect specific and keystone taxa representing “specialists” particularly well adapted to the presence of contaminants. Such “specialist” taxa, like *Hydrogenophaga*, *Ignavibacterium*, *Dechloromonas* and *Oscillatoria* represent potential bio-indicators or

"sentinels" to be included in integrative indices for evaluating the ecological status of aquatic environments. The network analysis showed that the microbial communities were organized in specialized modules around these "specialists" keystone taxa. The modules were tailored to respond specifically to the presence of a contaminant type, providing useful information to understand how the environmental parameters shape the organization of microbial assemblages. Particularly, *Nitrospira* was found to be an ideal partner for establishing microbial relationships under various conditions, which should be considered in environmental management. The results pave the way for future studies, particularly at the functional level, for deciphering the metabolic networks involved in the ecosystem functioning in estuarine ecosystems.

Acknowledgements

This work was financially supported by European Regional Development Fund (ERDF) and Agence de l'Eau Adour-Garonne (AEAG) grants in the framework of the MICROPOLIT project. The authors also acknowledge the support of EcosNord M15A01 project. The authors declare that they have no known competing financial interests or personal relationships that could have appeared to influence the work reported in this paper. Authors are grateful to Emmanuel Tessier, Aurore Gueux, Emna Zhegal, Andrea Romero Ramas, Alyssa Azaroff, Sandra Fauré, and Aurore Méré who helped in sediment samples collection and analysis.

Data Availability Statement

The sequencing datasets generated for this study are available at NCBI Sequence Read Archive (SRA) database under accession number **SUB9572817**.

Annex: **Supplementary material**

References

Abreu, C., Jurgens, G., De Marco, P., Saano, A., Bordalo, A.A., 2001. Crenarchaeota and euryarchaeota in temperate estuarine sediments. Journal of Applied Microbiology 90, 713–718. doi:10.1046/j.1365-2672.2001.01297.x

Aminot, Y., Le Menach, K., Pardon, P., Etcheber, H., Budzinski, H., 2016. Inputs and seasonal removal of pharmaceuticals in the estuarine Garonne River. Marine Chemistry 185, 3–11. doi:10.1016/j.marchem.2016.05.010

Aminot, A., Kérouel, R., 2004. Hydrologie des écosystèmes marins. Paramètres et analyses. Ifremer.

Anschutz, P., Bouchet, S., Abril, G., Bridou, R., Tessier, E., Amouroux, D., 2019. In vitro simulation of oscillatory redox conditions in intertidal sediments: N, Mn, Fe, and P coupling. Continental Shelf Research 177, 33–41. doi:10.1016/j.csr.2019.03.007

Aylagas, E., Borja, Á., Tangherlini, M., Dell'Anno, A., Corinaldesi, C., Michell, C.T., Irigoien, X., Danovaro, R., Rodríguez-Ezpeleta, N., 2017. A bacterial community-based index to assess the ecological status of estuarine and coastal environments. Marine Pollution Bulletin 114, 679–688. doi:10.1016/j.marpolbul.2016.10.050

Azaroff, A., Miossec, C., Lanceleur, L., Guyoneaud, R., Monperrus, M., 2020. Priority and emerging micropollutants distribution from coastal to continental slope sediments: A case study of Capbreton Submarine Canyon (North Atlantic Ocean). Science of The Total Environment 703, 135057. doi:10.1016/J.SCITOTENV.2019.135057

Bahram, M., Anslan, S., Hildebrand, F., Bork, P., Tedersoo, L., 2019. Newly designed 16S rRNA metabarcoding primers amplify diverse and novel archaeal taxa from the environment. Environmental Microbiology Reports 11, 487–494. doi:10.1111/1758-2229.12684

Baker-Austin, C., Wright, M.S., Stepanauskas, R., McArthur, J.V., 2006. Co-selection of antibiotic and metal resistance. Trends in Microbiology 14, 176–182. doi:10.1016/J.TIM.2006.02.006

Basset, A., Elliott, M., West, R.J., Wilson, J.G., 2013. Estuarine and lagoon biodiversity and their natural goods and services. Estuarine, Coastal and Shelf Science. doi:10.1016/j.ecss.2013.05.018

Bastian, M., Heymann, S., Jacomy, M., 2009. Gephi: An open source software for exploring and manipulating networks.

Bauer, J.E., Cai, W.J., Raymond, P.A., Bianchi, T.S., Hopkinson, C.S., Regnier, P.A.G., 2013. The changing carbon cycle of the coastal ocean. Nature 504, 61–70. doi:10.1038/nature12857

Ben Salem, F., Ben Said, O., Cravo-Laureau, C., Mahmoudi, E., Bru, N., Monperrus, M., Duran, R., 2019. Bacterial community assemblages in sediments under high anthropogenic pressure at Ichkeul Lake/Bizerte Lagoon hydrological system, Tunisia. Environmental Pollution 252, 644–656. doi:10.1016/j.envpol.2019.05.146

Ben Salem, F., Ben Said, O., Duran, R., Monperrus, M. 2016 Validation of an adapted QuEChERS method for the simultaneous analysis of polycyclic aromatic hydrocarbons, polychlorinated biphenyls and organochlorine pesticides in sediment by gas chromatography-mass spectrometry. Bulletin of Environmental Contamination and Toxicology 96: 678-684. doi:10.1007/s00128-016-1770-2

569 Boone, D.R., Castenholz, R.W., 2001. The *Archaea* and the deeply branching and phototrophic *Bacteria*,
570 in: Garrity, G.M. (Ed.), Bergey's Manual of Systematic Bacteriology. Springer, New-York, pp. 1–721.

571 Bordenave, S., Fourçans, A., Blanchard, S., Goñi, M.S., Caumette, P., Duran, R., 2004. Structure and
572 functional analyses of bacterial communities changes in microbial mats following petroleum exposure.
573 Ophelia 58, 195–203. doi:10.1080/00785236.2004.10410227

574 Breda, I.L., Ramsay, L., Roslev, P., 2017. Manganese oxidation and bacterial diversity on different filter
575 media coatings during the start-up of drinking water biofilters. Journal of Water Supply: Research and
576 Technology - AQUA 66, 641–650. doi:10.2166/aqua.2017.084

577 Bruneel, O., Pascault, N., Egal, M., Bancon-Montigny, C., Goñi-Urriza, M.S., Elbaz-Poulichet, F.,
578 Personné, J.C., Duran, R., 2008. Archaeal diversity in a Fe-As rich acid mine drainage at Carnoulès
579 (France). Extremophiles 12, 563–571. doi:10.1007/s00792-008-0160-z

580 Callahan, B.J., McMurdie, P.J., Rosen, M.J., Han, A.W., Johnson, A.J.A., Holmes, S.P., 2016a. DADA2:
581 High-resolution sample inference from Illumina amplicon data. Nature Methods 13, 581–583.
582 doi:10.1038/nmeth.3869

583 Callahan, B.J., Sankaran, K., Fukuyama, J.A., McMurdie, P.J., Holmes, S.P., 2016b. Bioconductor
584 Workflow for Microbiome Data Analysis: from raw reads to community analyses [version 2; peer review:
585 3 approved]. F1000Research 5, 1–50. doi:10.12688/f1000research.8986.2

586 Carmichael, M.J., Carmichael, S.K., Santelli, C.M., Strom, A., Bräuer, S.L., 2013. Mn(II)-oxidizing
587 Bacteria are Abundant and Environmentally Relevant Members of Ferromanganese Deposits in Caves of
588 the Upper Tennessee River Basin. Geomicrobiology Journal 30, 779–800.
589 doi:10.1080/01490451.2013.769651

590 Cavalheiro, J., Zuloaga, O., Prieto, A., Preudhomme, H., Amouroux, D., Monperrus, M., 2017.
591 Occurrence and Fate of Organic and Organometallic Pollutants in Municipal Wastewater Treatment Plants
592 and Their Impact on Receiving Waters (Adour Estuary, France). Archives of Environmental
593 Contamination and Toxicology 73, 619–630. doi:10.1007/s00244-017-0422-9

594 Cayrou, C., Raoult, D., Drancourt, M., 2010. Broad-spectrum antibiotic resistance of Planctomycetes
595 organisms determined by Etest. Journal of Antimicrobial Chemotherapy 65, 2119–2122.
596 doi:10.1093/jac/dkq290

597 Chakraborty, A., Miyahara, S., Villanueva, S.Y.A.M., Gloriani, N.G., Yoshida, S.I., 2010. In vitro
598 sensitivity and resistance of 46 Leptospira strains isolated from rats in the Philippines to 14 antimicrobial
599 agents. Antimicrobial Agents and Chemotherapy 54, 5403–5405. doi:10.1128/AAC.00973-10

600 Chen, C., Li, L., Huang, K., Zhang, J., Xie, W.Y., Lu, Y., Dong, X., Zhao, F.J., 2019. Sulfate-reducing
601 bacteria and methanogens are involved in arsenic methylation and demethylation in paddy soils. ISME
602 Journal 13, 2523–2535. doi:10.1038/s41396-019-0451-7

603 Chen, W.M., Chung, Y.N., Chiu, T.F., Cheng, C.Y., Arun, A.B., Sheu, S.Y., 2010. *Deefgea chitinilytica*
604 sp. nov., isolated from a wetland. International Journal of Systematic and Evolutionary Microbiology 60,
605 1450–1453. doi:10.1099/ijs.0.015263-0

606 Clauset, A., Newman, M.E.J., Moore, C., 2004. Finding community structure in very large networks.
607 Physical Review E - Statistical Physics, Plasmas, Fluids, and Related Interdisciplinary Topics 70, 066111.
608 doi:10.1103/PhysRevE.70.066111

Concha, C., Miranda, C.D., Rojas, R., Godoy, F.A., Romero, J., 2021. Characterization of a novel variant of the quinolone-resistance gene *qnrB* (*qnrB89*) carried by a multi-drug resistant *Citrobacter gillenii* strain isolated from farmed salmon in Chile. Antibiotics 10, 1–12. doi:10.3390/antibiotics10030236

Costa, F., Hagan, J.E., Calcagno, J., Kane, M., Torgerson, P., Martinez-Silveira, M.S., Stein, C., Abela-Ridder, B., Ko, A.I., 2015. Global Morbidity and Mortality of Leptospirosis: A Systematic Review. PLOS Neglected Tropical Diseases 9, e0003898. doi:10.1371/JOURNAL.PNTD.0003898

Costley, C.T., Mossop, K.F., Dean, J.R., Garden, L.M., Marshall, J., Carroll, J., 2000. Determination of mercury in environmental and biological samples using pyrolysis atomic absorption spectrometry with gold amalgamation. Analytica Chimica Acta 405, 179–183. doi:10.1016/S0003-2670(99)00742-4

Cravo-Laureau, C., Hernandez-Raquet, G., Vitte, I., Jézéquel, R., Bellet, V., Godon, J.J., Caumette, P., Balaguer, P., Duran, R., 2011. Role of environmental fluctuations and microbial diversity in degradation of hydrocarbons in contaminated sludge. Research in Microbiology 162, 888–895. doi:10.1016/j.resmic.2011.04.011

Crognale, S., Casentini, B., Amalfitano, S., Fazi, S., Petruccioli, M., Rossetti, S., 2019. Biological As(III) oxidation in biofilters by using native groundwater microorganisms. Science of the Total Environment 651, 93–102. doi:10.1016/j.scitotenv.2018.09.176

Cui, Y., Gao, J., Zhang, D., Li, D., Dai, H., Wang, Z., Zhao, Y., 2021. Responses of performance, antibiotic resistance genes and bacterial communities of partial nitrification system to polyamide microplastics. Bioresource Technology 341, 125767. doi:10.1016/j.biortech.2021.125767

Damashek, J., Francis, C.A., 2018. Microbial Nitrogen Cycling in Estuaries: From Genes to Ecosystem Processes. Estuaries and Coasts 41, 626–660. doi:10.1007/S12237-017-0306-2

Dehning, I., Schink, B., 1989. *Malonomonas rubra* gen. nov. sp. nov., a microaerotolerant anaerobic bacterium growing by decarboxylation of malonate. Archives of Microbiology 151, 427–433. doi:10.1007/BF00416602

Delépée, R., Pouliquen, H., Le Bris, H., 2004. The bryophyte *Fontinalis antipyretica* Hedw. bioaccumulates oxytetracycline, flumequine and oxolinic acid in the freshwater environment. Science of The Total Environment 322, 243–253. doi:10.1016/J.SCITOTENV.2003.09.018

Deng, Y., Jiang, Y.H., Yang, Y., He, Z., Luo, F., Zhou, J., 2012. Molecular ecological network analyses. BMC Bioinformatics 13. doi:10.1186/1471-2105-13-113

Dias, M., Salvado, J.C., Monperrus, M., Caumette, P., Amouroux, D., Duran, R., Guyoneaud, R., 2008. Characterization of *Desulfomicrobium salsuginis* sp. nov. and *Desulfomicrobium aestuarii* sp. nov., two new sulfate-reducing bacteria isolated from the Adour estuary (French Atlantic coast) with specific mercury methylation potentials. Systematic and Applied Microbiology 31, 30–37. doi:10.1016/j.syapm.2007.09.002

Duran, R., Bielen, A., Paradžik, T., Gassie, C., Pustijanac, E., Cagnon, C., Hamer, B., Vujaklija, D., 2015. Exploring Actinobacteria assemblages in coastal marine sediments under contrasted Human influences in the West Istria Sea, Croatia. Environmental Science and Pollution Research 22, 15215–15229. doi:10.1007/s11356-015-4240-1

Elliott, M., Quintino, V., 2007. The Estuarine Quality Paradox, Environmental Homeostasis and the difficulty of detecting anthropogenic stress in naturally stressed areas. Marine Pollution Bulletin 54, 640–645. doi:10.1016/j.marpolbul.2007.02.003

650 Fabbri, E., Franzellitti, S., 2016. Human pharmaceuticals in the marine environment: Focus on exposure
651 and biological effects in animal species. Environmental Toxicology and Chemistry 35, 799–812.
652 doi:10.1002/etc.3131

653 Feng, B.W., Li, X.R., Wang, J.H., Hu, Z.Y., Meng, H., Xiang, L.Y., Quan, Z.X., 2009. Bacterial diversity
654 of water and sediment in the Changjiang estuary and coastal area of the East China Sea. FEMS
655 Microbiology Ecology 70, 236–248. doi:10.1111/j.1574-6941.2009.00772.x

656 Fernández-Gómez, B., Richter, M., Schüler, M., Pinhassi, J., Acinas, S.G., González, J.M., Pedrós-Alió,
657 C., 2013. Ecology of marine bacteroidetes: A comparative genomics approach. ISME Journal 7, 1026–
658 1037. doi:10.1038/ismej.2012.169

659 Fortunato, C.S., Crump, B.C., 2015. Microbial gene abundance and expression patterns across a river to
660 ocean salinity gradient. PLoS ONE 10, 1–22. doi:10.1371/journal.pone.0140578

661 Fuhrman, J.A., Steele, J.A., 2008. Community structure of marine bacterioplankton: Patterns, networks,
662 and relationships to function, in: Aquatic Microbial Ecology. pp. 69–81. doi:10.3354/ame01222

663 Gerasimenko, L.M., Orleanskii, V.K., Zaitseva, L.V., 2013. Accumulation and precipitation of Mn^{2+} by
664 the cells of *Oscillatoria terebriformis*. Microbiology 82, 609–617. doi:10.1134/S0026261713050032

665 Gerzova, L., Videnska, P., Faldynova, M., Sedlar, K., Provaznik, I., Cizek, A., Rychlik, I., 2014.
666 Characterization of microbiota composition and presence of selected antibiotic resistance genes in carriage
667 water of ornamental fish. PLoS ONE 9, e103865. doi:10.1371/journal.pone.0103865

668 Giloteaux, L., Duran, R., Casiot, C., Bruneel, O., Elbaz-Poulichet, F., Goñi-Urriza, M., 2013. Three-year
669 survey of sulfate-reducing bacteria community structure in Carnoulès acid mine drainage (France), highly
670 contaminated by arsenic. FEMS Microbiology Ecology 83, 724–737. doi:10.1111/1574-6941.12028

671 Godinho, O., Calisto, R., Øvreås, L., Quinteira, S., Lage, O.M., 2019. Antibiotic susceptibility of marine
672 *Planctomycetes*. Antonie van Leeuwenhoek 112, 1273–1280. doi:10.1007/s10482-019-01259-7

673 Gros, M., Blum, K.M., Jernstedt, H., Renman, G., Rodríguez-Mozaz, S., Haglund, P., Andersson, P.L.,
674 Wiberg, K., Ahrens, L., 2017. Screening and prioritization of micropollutants in wastewaters from on-site
675 sewage treatment facilities. Journal of Hazardous Materials 328, 37–45.
676 doi:10.1016/j.jhazmat.2016.12.055

677 Guironnet, A., Wiest, L., Vulliet, E., 2022. Improvement of the QuEChERS extraction step by matrix-
678 dispersion effect and application on beta-lactams analysis in wastewater sludge by LC-MS/MS. Talanta
679 237, 122923. doi:10.1016/J.TALANTA.2021.122923

680 Guo, X., Lu, D., Niu, Z., Feng, J., Chen, Y., Tou, F., Liu, M., Yang, Y., 2018. Bacterial community
681 structure in response to environmental impacts in the intertidal sediments along the Yangtze Estuary,
682 China. Marine Pollution Bulletin 126, 141–149. doi:10.1016/j.marpolbul.2017.11.003

683 Guo, X., Yang, Y., Niu, Z. shun, Lu, D.P., Zhu, C. hong, Feng, J. nan, Wu, J. yuan, Chen, Y. ru, Tou, F.
684 yun, Liu, M., Hou, L., 2019. Characteristics of microbial community indicate anthropogenic impact on the
685 sediments along the Yangtze Estuary and its coastal area, China. Science of the Total Environment 648,
686 306–314. doi:10.1016/j.scitotenv.2018.08.162

687 Han, S., Huang, Q., Chen, W., 2021. Partitioning *Nitrospira* community structure and co-occurrence
688 patterns in a long-term inorganic and organic fertilization soil. Journal of Soils and Sediments 21, 1099–
689 1108. doi:10.1007/s11368-020-02813-x

He, K., Hain, E., Timm, A., Tarnowski, M., Blaney, L., 2019. Occurrence of antibiotics, estrogenic hormones, and UV-filters in water, sediment, and oyster tissue from the Chesapeake Bay. Science of the Total Environment 650, 3101–3109. doi:10.1016/j.scitotenv.2018.10.021

Iino, T., Mori, K., Uchino, Y., Nakagawa, T., Harayama, S., Suzuki, K.I., 2010. *Ignavibacterium album* gen. nov., sp. nov., a moderately thermophilic anaerobic bacterium isolated from microbial mats at a terrestrial hot spring and proposal of *Ignavibacteria* classis nov., for a novel lineage at the periphery of green sulfur bacteria. International Journal of Systematic and Evolutionary Microbiology 60, 1376–1382. doi:10.1099/ijs.0.012484-0

Islam, F.S., Boothman, C., Gault, A.G., Polya, D.A., Lloyd, J.R., 2005. Potential role of the Fe(III) reducing bacteria Geobacter and Geothrix in controlling arsenic solubility in Bengal delta sediments. Mineralogical Magazine 69, 865–875. doi:10.1180/0026461056950294

Jabari, L., Gannoun, H., Cayol, J.L., Hedi, A., Sakamoto, M., Falsen, E., Ohkuma, M., Hamdi, M., Fauque, G., Ollivier, B., Fardeau, M.L., 2012. *Macellibacteroides fermentans* gen. nov., sp. nov., a member of the family *Porphyromonadaceae* isolated from an upflow anaerobic filter treating abattoir wastewaters. International Journal of Systematic and Evolutionary Microbiology 62, 2522–2527. doi:10.1099/ijs.0.032508-0

Jacquiod, S., Cyriaque, V., Riber, L., Al-soud, W.A., Gillan, D.C., Wattiez, R., Sørensen, S.J., 2018. Long-term industrial metal contamination unexpectedly shaped diversity and activity response of sediment microbiome. Journal of Hazardous Materials 344, 299–307. doi:10.1016/j.jhazmat.2017.09.046

Jauregi, L., Epelde, L., Alkorta, I., Garbisu, C., 2021. Agricultural Soils Amended With Thermally-Dried Anaerobically-Digested Sewage Sludge Showed Increased Risk of Antibiotic Resistance Dissemination. Frontiers in Microbiology 12, 955. doi:10.3389/fmicb.2021.666854

Jeanbille, M., Gury, J., Duran, R., Tronczynski, J., Agogué, H., Ben Saïd, O., Ghiglione, J.-F., Auguet, J.-C., 2016. Response of Core Microbial Consortia to Chronic Hydrocarbon Contaminations in Coastal Sediment Habitats. Frontiers in Microbiology 7, 1–13. doi:10.3389/fmicb.2016.01637

Jiang, L.Q., Zhang, K., Li, G.D., Wang, X.Y., Shi, S.B., Li, Q.Y., An, D.F., Lang, L., Wang, L.S., Jiang, C.L., Jiang, Y., 2019. *Rubellimicrobium rubrum* sp. nov., a novel bright reddish bacterium isolated from a lichen sample. Antonie van Leeuwenhoek 112, 1739–1745. doi:10.1007/S10482-019-01304-5

Johnston, E.L., Roberts, D.A., 2009. Contaminants reduce the richness and evenness of marine communities: A review and meta-analysis. Environmental Pollution 157, 1745–1752. doi:10.1016/j.envpol.2009.02.017

Kaci, A., Petit, F., Fournier, M., Cécillon, S., Boust, D., Lesueur, P., Berthe, T., 2016. Diversity of active microbial communities subjected to long-term exposure to chemical contaminants along a 40-year-old sediment core. Environmental Science and Pollution Research 23, 4095–4110. doi:10.1007/s11356-015-4506-7

Kashefi, K., Holmes, D.E., Baross, J.A., Lovley, D.R., 2003. Thermophily in the *Geobacteraceae*: *Geothermobacter ehrlichii* gen. nov., sp. nov., a novel thermophilic member of the *Geobacteraceae* from the "Bag City" hydrothermal vent. Applied and Environmental Microbiology 69, 2985–2993. doi:10.1128/AEM.69.5.2985-2993.2003

Kennish, M.J., 2002. Environmental threats and environmental future of estuaries. Environmental Conservation 29, 78–107. doi:10.1017/S0376892902000061

Kirchman, D.L., 2002. The ecology of *Cytophaga-Flavobacteria* in aquatic environments. FEMS Microbiology Ecology 39, 91–100. doi:10.1111/j.1574-6941.2002.tb00910.x

Kisand, V., Cuadros, R., Wikner, J., 2002. Phylogeny of culturable estuarine bacteria catabolizing riverine organic matter in the northern Baltic Sea. Applied and Environmental Microbiology 68, 379–388. doi:10.1128/AEM.68.1.379-388.2002

Kubo, A., Kanda, J., 2017. Seasonal variations and sources of sedimentary organic carbon in Tokyo Bay. Marine Pollution Bulletin 114, 637–643. doi:10.1016/J.MARPOLBUL.2016.10.030

Lanceleur, L., Schäfer, J., Bossy, C., Coynel, A., Larrose, A., Masson, M., Blanc, G., 2011. Silver fluxes to the Gironde Estuary - Eleven years (1999-2009) of monitoring at the watershed scale. Applied Geochemistry 26, 797–808. doi:10.1016/J.APGEOCHEM.2011.02.001

Li, C., Quan, Q., Gan, Y., Dong, J., Fang, J., Wang, L., Liu, J., 2020. Effects of heavy metals on microbial communities in sediments and establishment of bioindicators based on microbial taxa and function for environmental monitoring and management. Science of the Total Environment 749, 1–9. doi:10.1016/j.scitotenv.2020.141555

Li, F., Huang, Y., Hu, W., Li, Z., Wang, Q., Huang, S., Jiang, F., Pan, X., 2021. *Roseomonas coralli* sp. Nov., a heavy metal resistant bacterium isolated from coral. International Journal of Systematic and Evolutionary Microbiology 71, 1–7. doi:10.1099/ijsem.0.004624

Li, X., Wan, W., Zheng, L., Wang, A., Luo, X., Huang, Q., Chen, W., 2021. Community assembly mechanisms and co-occurrence patterns of nitrite-oxidizing bacteria communities in saline soils. Science of the Total Environment 772. doi:10.1016/j.scitotenv.2021.145472

Li, Z., Sobek, A., Radke, M., 2016. Fate of Pharmaceuticals and Their Transformation Products in Four Small European Rivers Receiving Treated Wastewater. Environmental Science and Technology 50, 5614–5621. doi:10.1021/acs.est.5b06327

Liu, J.L., Wong, M.H., 2013. Pharmaceuticals and personal care products (PPCPs): A review on environmental contamination in China. Environment International 59, 208–224. doi:10.1016/j.envint.2013.06.012

Liu, J., Yao, J., Zhu, X., Zhou, D. liang, Duran, R., Mihucz, V.G., Bashir, S., Hudson-Edwards, K.A., 2021. Metagenomic exploration of multi-resistance genes linked to microbial attributes in active nonferrous metal(loid) tailings. Environmental Pollution 273, 115667. doi:10.1016/j.envpol.2020.115667

Liu, X., Pan, J., Liu, Y., Li, M., Gu, J.D., 2018. Diversity and distribution of Archaea in global estuarine ecosystems. Science of the Total Environment 637-638, 349–358. doi:10.1016/j.scitotenv.2018.05.016

Liu, Z., Lin, S., Piantadosi, S., 2015. Network construction and structure detection with metagenomic count data. BioData Mining 8, 1–14. doi:10.1186/s13040-015-0072-2

Lladó, S., Covino, S., Solanas, A.M., Petruccioli, M., D'annibale, A., Viñas, M., 2015. Pyrosequencing reveals the effect of mobilizing agents and lignocellulosic substrate amendment on microbial community composition in a real industrial PAH-polluted soil. Journal of Hazardous Materials 283, 35–43. doi:10.1016/j.jhazmat.2014.08.065

Lorenzen, C.J., 1967. Determination of chlorophyll and pheo-pigments: Spectrophotometric equations. Limnology and Oceanography 60th Anniversary Special Collection 12, 343–346. doi:10.4319/lo.1967.12.2.0343

Lozupone, C.A., Knight, R., 2007. Global patterns in bacterial diversity. Proceedings of the National Academy of Sciences 104, 11436–11440. doi:10.1073/pnas.0611525104

Mailler, R., Gasperi, J., Patureau, D., Vulliet, E., Delgenes, N., Danel, A., Deshayes, S., Eudes, V., Guerin, S., Moilleron, R., Chebbo, G., Rocher, V., 2017. Fate of emerging and priority micropollutants during the sewage sludge treatment: Case study of Paris conurbation. Part 1: Contamination of the different types of sewage sludge. Waste Management 59, 379–393. doi:10.1016/j.wasman.2016.11.010

McGenity, T.J., Folwell, B.D., McKew, B.A., Sanni, G.O., 2012. Marine crude-oil biodegradation: a central role for interspecies interactions. Aquatic Biosystems 8, 1–19. doi:10.1186/2046-9063-8-10

Mehrani, M.J., Sobotka, D., Kowal, P., Ciesielski, S., Makinia, J., 2020. The occurrence and role of *Nitrospira* in nitrogen removal systems. Bioresource Technology 303, 122936. doi:10.1016/j.biortech.2020.122936

Mei, R., Nobu, M.K., Narihiro, T., Liu, W.-T., 2020. Metagenomic and Metatranscriptomic Analyses Revealed Uncultured Bacteroidales Populations as the Dominant Proteolytic Amino Acid Degraders in Anaerobic Digesters. Frontiers in Microbiology 11, 2763. doi:10.3389/fmicb.2020.593006

Meng, L., Liu, H., Lan, T., Dong, L., Hu, H., Zhao, S., Zhang, Y., Zheng, N., Wang, J., 2020. Antibiotic Resistance Patterns of *Pseudomonas* spp. Isolated From Raw Milk Revealed by Whole Genome Sequencing. Frontiers in Microbiology 11, 1–10. doi:10.3389/fmicb.2020.01005

Misson, B., Garnier, C., Lauga, B., Dang, D.H., Ghiglione, J.F., Mullot, J.U., Duran, R., Pringault, O., 2016. Chemical multi-contamination drives benthic prokaryotic diversity in the anthropized Toulon Bay. Science of the Total Environment 556, 319–329. doi:10.1016/j.scitotenv.2016.02.038

Molari, M., Janssen, F., Vonnahme, T.R., Wenzhöfer, F., Boetius, A., 2020. The contribution of microbial communities in polymetallic nodules to the diversity of the deep-sea microbiome of the Peru Basin (4130-4198m depth). Biogeosciences 17, 3203–3222. doi:10.5194/bg-17-3203-2020

Murali, A., Bhargava, A., Wright, E.S., 2018. IDTAXA: A novel approach for accurate taxonomic classification of microbiome sequences. Microbiome 6. doi:10.1186/s40168-018-0521-5

Nakagawa, S., Takai, K., Inagaki, F., Hirayama, H., Nunoura, T., Horikoshi, K., Sako, Y., 2005. Distribution, phylogenetic diversity and physiological characteristics of epsilon-*Proteobacteria* in a deep-sea hydrothermal field. Environmental Microbiology 7, 1619–1632. doi:10.1111/j.1462-2920.2005.00856.x

Newman, M.E.J., 2004. Fast algorithm for detecting community structure in networks. Physical Review E - Statistical Physics, Plasmas, Fluids, and Related Interdisciplinary Topics 69, 066133. doi:10.1103/PhysRevE.69.066133

Obimakinde, S., Fatoki, O., Opeolu, B., Olatunji, O., 2017. Veterinary pharmaceuticals in aqueous systems and associated effects: an update. Environmental Science and Pollution Research 24, 3274–3297. doi:10.1007/s11356-016-7757-z

Oksanen, J., Blanchet, F.G., Friendly, M., Kindt, R., Legendre, P., McGlinn, D., Minchin, P.R., O'Hara, R.B., Simpson, G.L., Solymos, P., Stevens, M.H.H., Szoecs, E., Wagner, H., 2020. vegan: Community ecology package. https://github.com/vegandevs/vegan

Paissé, S., Coulon, F., Goñi-Urriza, M., Peperzak, L., McGenity, T.J., Duran, R., 2008. Structure of bacterial communities along a hydrocarbon contamination gradient in a coastal sediment. FEMS Microbiology Ecology 66, 295–305. doi:10.1111/j.1574-6941.2008.00589.x

812 Palomo, A., Jane Fowler, S., Gülay, A., Rasmussen, S., Sicheritz-Ponten, T., Smets, B.F., 2016.
813 Metagenomic analysis of rapid gravity sand filter microbial communities suggests novel physiology of
814 *Nitrospira* spp. ISME Journal 10, 2569–2581. doi:10.1038/ismej.2016.63

815 Palomo, A., Pedersen, A.G., Fowler, S.J., Dechesne, A., Sicheritz-Pontén, T., Smets, B.F., 2018.
816 Comparative genomics sheds light on niche differentiation and the evolutionary history of comammox
817 *Nitrospira*. ISME Journal 12, 1779–1793. doi:10.1038/s41396-018-0083-3

818 Parada, A.E., Needham, D.M., Fuhrman, J.A., 2016. Every base matters: Assessing small subunit rRNA
819 primers for marine microbiomes with mock communities, time series and global field samples.
820 Environmental Microbiology 18, 1403–1414. doi:10.1111/1462-2920.13023

821 Pascual, J., García-López, M., González, I., Genilloud, O., 2017. *Luteolibacter gellanilyticus* sp. Nov., a
822 gellan-gum-degrading bacterium of the phylum *Verrucomicrobia* isolated from miniaturized diffusion
823 chambers. International Journal of Systematic and Evolutionary Microbiology 67, 3951–3959.
824 doi:10.1099/ijsem.0.002227

825 Persuad, D., Jaagumagi, R., Hayton, A., 1993. Guidelines for the protection and management of aquatic
826 sediment quality in Ontario. Ontario Ministry of the Environment, Canada

827 Petrovski, S., Rice, D.T.F., Batinovic, S., Nittami, T., Seviour, R.J., 2020. The community compositions
828 of three nitrogen removal wastewater treatment plants of different configurations in Victoria, Australia,
829 over a 12-month operational period. Applied Microbiology and Biotechnology 104, 9839–9852.
830 doi:10.1007/s00253-020-10901-8

831 Peysson, W., Vulliet, E., 2013. Determination of 136 pharmaceuticals and hormones in sewage sludge
832 using quick, easy, cheap, effective, rugged and safe extraction followed by analysis with liquid
833 chromatography–time-of-flight-mass spectrometry. Journal of Chromatography A 1290, 46–61.
834 doi:10.1016/J.CHROMA.2013.03.057

835 Point, D., 2004. Spéciation et biogéochimie des éléments traces métalliques dans l'estuaire de l'Adour.
836 (PhD Thesis). Université de Pau et des Pays de l'Adour.

837 Pommier, T., Canbäck, B., Riemann, L., Boström, K.H., Simu, K., Lundberg, P., Tunlid, A., Hagström,
838 Å., 2007. Global patterns of diversity and community structure in marine bacterioplankton. Molecular
839 Ecology 16, 867–880. doi:10.1111/j.1365-294X.2006.03189.x

840 Pringault, O., Duran, R., Jacquet, S., Torréton, J.P., 2008. Temporal variations of microbial activity and
841 diversity in marine tropical sediments (New Caledonia Lagoon). Microbial Ecology 55, 247–258.
842 doi:10.1007/s00248-007-9272-8

843 Pringault, O., Viret, H., Duran, R., 2010. Influence of microorganisms on the removal of nickel in tropical
844 marine sediments (New Caledonia). Marine Pollution Bulletin 61, 530–541.
845 doi:10.1016/j.marpolbul.2010.06.038

846 Pringault, O., Viret, H., Duran, R., 2012. Interactions between Zn and bacteria in marine tropical coastal
847 sediments. Environmental Science and Pollution Research 19, 879–892. doi:10.1007/s11356-011-0621-2

848 Qi, X.e., Wang, C., He, T., Ding, F., Li, A., Zhang, X., An, L., Xu, S., 2021. Changes in alpine grassland
849 type drive niche differentiation of nitrifying communities on the Qinghai–Tibetan Plateau. European
850 Journal of Soil Biology 104, 103316. doi:10.1016/j.ejsobi.2021.103316

Quadra, G.R., Paranaíba, J.R., Vilas-Boas, J., Roland, F., Amado, A.M., Barros, N., Dias, R.J.P., Cardoso, S.J., 2020. A global trend of caffeine consumption over time and related-environmental impacts. Environmental Pollution 256, 113343. doi:10.1016/j.envpol.2019.113343

Quast, C., Pruesse, E., Yilmaz, P., Gerken, J., Schweer, T., Yarza, P., Peplies, J., Glöckner, F.O., 2013. The SILVA ribosomal RNA gene database project: Improved data processing and web-based tools. Nucleic Acids Research 41, D590–D596. doi:10.1093/nar/gks1219

Quince, C., Lanzen, A., Davenport, R.J., Turnbaugh, P.J., 2011. Removing Noise From Pyrosequenced Amplicons. BMC Bioinformatics 12, 38. doi:10.1186/1471-2105-12-38

R Core Team, 2020. R: A Language and Environment for Statistical Computing. R Foundation for Statistical Computing. https://www.r-project.org

Roberto, A.A., Van Gray, J.B., Leff, L.G., 2018. Sediment bacteria in an urban stream: Spatiotemporal patterns in community composition. Water Research 134, 353–369. doi:10.1016/j.watres.2018.01.045

Rodriguez-Mozaz, S., Vaz-Moreira, I., Varela Della Giustina, S., Llorca, M., Barceló, D., Schubert, S., Berendonk, T.U., Michael-Kordatou, I., Fatta-Kassinos, D., Martinez, J.L., Elpers, C., Henriques, I., Jaeger, T., Schwartz, T., Paulshus, E., O'Sullivan, K., Pärnänen, K.M.M., Virta, M., Do, T.T., Walsh, F., Manaia, C.M., 2020. Antibiotic residues in final effluents of European wastewater treatment plants and their impact on the aquatic environment. Environment International 140, 105733. doi:10.1016/j.envint.2020.105733

Saitoh, S., Suzuki, T., Nishimura, Y., 1998. Proposal of *Craurococcus roseus* gen. nov., sp. nov. and *Paracraurococcus ruber* gen. nov., sp. nov., novel aerobic bacteriochlorophyll a-containing bacteria from soil. International Journal of Systematic Bacteriology 48, 1043–1047. doi:10.1099/00207713-48-3-1043

Savoye, N., David, V., Morisseau, F., Etcheber, H., Abril, G., Billy, I., Charlier, K., Oggian, G., Derriennic, H., Sautour, B., 2012. Origin and composition of particulate organic matter in a macrotidal turbid estuary: The Gironde Estuary, France. Estuarine, Coastal and Shelf Science 108, 16–28. doi:10.1016/j.ecss.2011.12.005

Schink, B., Pfennig, N., 1982. *Propionigenium modestum* gen. nov. sp. nov. a new strictly anaerobic, nonsporing bacterium growing on succinate. Archives of Microbiology 133, 209–216. doi:10.1007/BF00415003

Schumann, P., Pukall, R., 2017. *Leucobacter weissii* sp. Nov., an isolate from activated sludge once described as first representative of the peptidoglycan variation B2δ, and emended description of the genus *Leucobacter*. International Journal of Systematic and Evolutionary Microbiology 67, 5244–52351. doi:10.1099/ijsem.0.002454

She, C.X., Zhang, Z.C., Cadillo-Quiroz, H., Tong, C., 2016. Factors regulating community composition of methanogens and sulfate-reducing bacteria in brackish marsh sediments in the Min River estuary, southeastern China. Estuarine, Coastal and Shelf Science 181, 27–38. doi:10.1016/j.ecss.2016.08.003

Shi, H., Yang, Y., Liu, M., Yan, C., Yue, H., Zhou, J., 2014. Occurrence and distribution of antibiotics in the surface sediments of the Yangtze Estuary and nearby coastal areas. Marine Pollution Bulletin. doi:10.1016/j.marpolbul.2014.04.034

Siedlewicz, G., Borecka, M., Białk-Bielińska, A., Sikora, K., Stepnowski, P., Pazdro, K., 2016. Determination of antibiotic residues in southern Baltic Sea sediments using tandem solid-phase extraction

and liquid chromatography coupled with tandem mass spectrometry. Oceanologia 58, 221–234. doi:10.1016/J.OCEANO.2016.04.005

Stoichev, T., Amouroux, D., Wasserman, J.C., Point, D., De Diego, A., Bareille, G., Donard, O.F.X., 2004. Dynamics of mercury species in surface sediments of a macrotidal estuarine-coastal system (Adour River, Bay of Biscay). Estuarine, Coastal and Shelf Science 59, 511–521. doi:10.1016/j.ecss.2003.10.007

Stroud, J.L., Low, A., Collins, R.N., Manefield, M., 2014. Metal(loid) bioaccessibility dictates microbial community composition in acid sulfate soil horizons and sulfidic drain sediments. Environmental Science and Technology 48, 8514–8521. doi:10.1021/es501495s

Su, X.L., Tian, Q., Zhang, J., Yuan, X.Z., Shi, X.S., Guo, R.B., Qiu, Y.L., 2014. *Acetobacteroides hydrogenigenes* gen. nov., Sp. nov., An anaerobic hydrogen-producing bacterium in the family *Rikenellaceae* isolated from a reed swamp. International Journal of Systematic and Evolutionary Microbiology 64, 2986–2991. doi:10.1099/ijs.0.063917-0

Suhadolnik, M.L.S., Salgado, A.P.C., Scholte, L.L.S., Bleicher, L., Costa, P.S., Reis, M.P., Dias, M.F., Ávila, M.P., Barbosa, F.A.R., Chartone-Souza, E., Nascimento, A.M.A., 2017. Novel arsenic-transforming bacteria and the diversity of their arsenic-related genes and enzymes arising from arsenic-polluted freshwater sediment. Scientific Reports 7, 1–17. doi:10.1038/s41598-017-11548-8

Sun, M.Y., Dafforn, K.A., Brown, M.V., Johnston, E.L., 2012. Bacterial communities are sensitive indicators of contaminant stress. Marine Pollution Bulletin 64, 1029–1038. doi:10.1016/j.marpolbul.2012.01.035

Sun, Y., Feng, Z., Tomura, T., Suzuki, A., Miyano, S., Tsuge, T., Mori, H., Suh, J.W., Iizuka, T., Fudou, R., Ojika, M., 2016. Heterologous Production of the Marine Myxobacterial Antibiotic Haliangicin and Its Unnatural Analogues Generated by Engineering of the Biochemical Pathway. Scientific Reports 6, 1–11. doi:10.1038/srep22091

Szabó, E., Liébana, R., Hermansson, M., Modin, O., Persson, F., Wilén, B.M., 2017. Microbial population dynamics and ecosystem functions of anoxic/aerobic granular sludge in sequencing batch reactors operated at different organic loading rates. Frontiers in Microbiology 8. doi:10.3389/fmicb.2017.00770

Vercraene-Eairmal, M., Lauga, B., Saint Laurent, S., Mazzella, N., Boutry, S., Simon, M., Karama, S., Delmas, F., Duran, R., 2010. Diuron biotransformation and its effects on biofilm bacterial community structure. Chemosphere 81, 837–843. doi:10.1016/j.chemosphere.2010.08.014

Vidal-Durà, A., Burke, I.T., Mortimer, R.J.G., Stewart, D.I., 2018. Diversity patterns of benthic bacterial communities along the salinity continuum of the Humber estuary (UK). Aquatic Microbial Ecology 81, 277–291. doi:10.3354/ame01875

Waite, D.W., Chuvochina, M., Pelikan, C., Parks, D.H., Yilmaz, P., Wagner, M., Loy, A., Naganuma, T., Nakai, R., Whitman, W.B., Hahn, M.W., Kuever, J., Hugenholtz, P., 2020. Proposal to reclassify the proteobacterial classes *Deltaproteobacteria* and *Oligoflexia*, and the phylum *Thermodesulfobacteria* into four phyla reflecting major functional capabilities. International Journal of Systematic and Evolutionary Microbiology 70, 5972–6016. doi:https://doi.org/10.1099/ijsem.0.004213

Wan, X., Gao, Q., Zhao, J., Feng, J., Nostrand, J.D. van, Yang, Y., Zhou, J., 2020. Biogeographic patterns of microbial association networks in paddy soil within Eastern China. Soil Biology and Biochemistry 142, 107696. doi:10.1016/j.soilbio.2019.107696

Wang, F., Dong, W., Zhao, Z., Wang, H., Li, W., Chen, G., Wang, F., Zhao, Y., Huang, J., Zhou, T., 2021. Heavy metal pollution in urban river sediment of different urban functional areas and its influence on microbial community structure. Science of the Total Environment 778. doi:10.1016/j.scitotenv.2021.146383

Wang, H., Li, J., Zheng, T., Hill, R.T., Hu, X., 2013. *Imperialibacter roseus* gen. nov., sp. nov., a novel bacterium of the family *Flammeovirgaceae* isolated from Permian groundwater. International journal of systematic and evolutionary microbiology 63, 4136–4140. doi:10.1099/IJS.0.052662-0

Wang, L., Liu, L., Zheng, B., Zhu, Y., Wang, X., 2013. Analysis of the bacterial community in the two typical intertidal sediments of Bohai Bay, China by pyrosequencing. Marine Pollution Bulletin 72, 181–187. doi:10.1016/j.marpolbul.2013.04.005

Wang, M., Sha, C., Wu, J., Su, J., Wu, J., Wang, Q., Tan, J., Huang, S., 2021. Bacterial community response to petroleum contamination in brackish tidal marsh sediments in the Yangtze River Estuary, China. Journal of Environmental Sciences 99, 160–167. doi:10.1016/j.jes.2020.06.015

Wang, X., Lu, L., Zhou, X., Tang, X., Kuang, L., Chen, J., Shan, J., Lu, H., Qin, H., Adams, J., Wang, B., 2021. Niche Differentiation of Comammox *Nitrospira* in the Mudflat and Reclaimed Agricultural Soils Along the North Branch of Yangtze River Estuary. Frontiers in Microbiology 11. doi:10.3389/fmicb.2020.618287

Watson, S.J., Cade-Menun, B.J., Needoba, J.A., Peterson, T.D., 2018. Phosphorus Forms in Sediments of a River-Dominated Estuary. Frontiers in Marine Science 5. doi:10.3389/fmars.2018.00302

Webster, G., O'Sullivan, L.A., Meng, Y., Williams, A.S., Sass, A.M., Watkins, A.J., Parkes, R.J., Weightman, A.J., 2015. Archaeal community diversity and abundance changes along a natural salinity gradient in estuarine sediments. FEMS Microbiology Ecology 91, 1–18. doi:10.1093/femsec/fiu025

Wen, K., Zhou, A., Zhang, J., Liu, Z., Wang, G., Liu, W., Wang, A., Yue, X., 2017. Characterization of biocarbon-source recovery and microbial community shifts from waste activated sludge by conditioning with cornstover: Assessment of cellulosic compositions. Scientific Reports 7, 1–11. doi:10.1038/srep42887

Willems, A., 2014. The family *Comamonadaceae*, in: Rosenberg, E., DeLong, E.F., Lory, S., Stackebrandt, E., Thompson, F. (Eds.), The Prokaryotes: Alphaproteobacteria and Betaproteobacteria. Springer Berlin Heidelberg, pp. 777–851. doi:10.1007/978-3-642-30197-1_238

Williams, R.J., Howe, A., Hofmockel, K.S., 2014. Demonstrating microbial co-occurrence pattern analyses within and between ecosystems. Frontiers in Microbiology 5, 358. doi:10.3389/fmicb.2014.00358

Xia, N., Xia, X., Zhu, B., Zheng, S., Zhuang, J., 2013. Bacterial diversity and community structure in the sediment of the middle and lower reaches of the Yellow River, the largest turbid river in the world. Aquatic Microbial Ecology 71, 43–55. doi:10.3354/ame01664

Yan, Y.W., Jiang, Q.Y., Wang, J.G., Zhu, T., Zou, B., Qiu, Q.F., Quan, Z.X., 2018. Microbial communities and diversities in mudflat sediments analyzed using a modified metatranscriptomic method. Frontiers in Microbiology 9. doi:10.3389/fmicb.2018.00093

Yi, J., Lo, L.S.H., Cheng, J., 2020. Dynamics of Microbial Community Structure and Ecological Functions in Estuarine Intertidal Sediments. Frontiers in Marine Science 7, 1–15. doi:10.3389/fmars.2020.585970

Yin, H., Niu, J., Ren, Y., Cong, J., Zhang, X.X., Fan, F., Xiao, Y., Zhang, X.X., Deng, J., Xie, M., He, Z., Zhou, J., Liang, Y., Liu, X., 2015. An integrated insight into the response of sedimentary microbial communities to heavy metal contamination. Scientific Reports 5, 1–12. doi:10.1038/srep14266

Zhang, Q., Zhang, Z., Lu, T., Peijnenburg, W.J.G.M., Gillings, M., Yang, X., Chen, J., Penuelas, J., Zhu, Y.G., Zhou, N.Y., Su, J., Qian, H., 2020. Cyanobacterial blooms contribute to the diversity of antibiotic-resistance genes in aquatic ecosystems. Communications Biology 3, 1–10. doi:10.1038/s42003-020-01468-1

Zhou, J., Deng, Y., Luo, F., He, Z., Yanga, Y., 2011. Phylogenetic molecular ecological network of soil microbial communities in response to elevated CO_2. mBio 2. doi:10.1128/mBio.00122-11

Zinger, L., Amaral-Zettler, L.A., Fuhrman, J.A., Horner-Devine, M.C., Huse, S.M., Welch, D.B.M., Martiny, J.B.H., Sogin, M., Boetius, A., Ramette, A., 2011. Global patterns of bacterial beta-diversity in seafloor and seawater ecosystems. PLoS ONE 6. doi:10.1371/journal.pone.0024570

Figure captions

Fig. 1. Sampling area and site location along the Adour Estuary. Sites are identified by numbers and colors. Shapes indicate site position along the estuary, (■) upstream, (●) middle and (▲) downstream.

Fig. 2. Comparison of Adour Estuary sites based on hydrological and geochemical parameters and pollutants content. PCA for (A) sites discriminating by sampling season and site position, and (B) variables including metals (red), pharmaceuticals (purple), geochemical parameters (blue) concentrations and abiotic parameters (black).

Fig. 3. Microbial community composition. Relative abundance (average of three replicates) of dominant microbial groups (phylum, class or order) observed by site and season in Adour Estuary sediment. NA, not assigned sequences; Other, taxa with abundance below 0.2% for phyla and classes and 1 % for orders.

Fig. 4. Comparison of microbial community composition. A) Hierarchical clustering based on Bray-Curtis dissimilarity computed on ASVs composition using the Ward D2 linkage method. The analysis was performed on the average of three replicates. The four groups were determined according to the explained inertia (83% with four groups). The seasons are identified by colors: spring (green), summer (pink) and winter (yellow). B) NMDS showing k-means clusters, based on the Bray-Curtis distances with samples pooled by site (without taking account to the season).

Fig. 5. Correlations between microbial community structures (genus level) with the environmental chemical parameters by CCA. The sites, the chemicals (arrows), and the ASVs at the genus level (grey points) are plotted. The bacterial genera discussed in the text are shown in red.

Fig. 6. Adour sediments microbial communities network analysis. (A) Global network representation where each node corresponds to an ASV, node size is proportional to the node betweenness. Networks are first colored according to phylum (A1) where NA, designated not assigned sequences and Other, phyla with abundance below 1%. Or, they are colored by (A2) modules, where modules significantly positively correlated with environmental parameters

selected are identified in colors and Others designed nodes that does not belong to these modules. (B) Heatmap of correlation between modules and environmental variables indicating Spearman correlation values (p-value). Only correlation with p-value higher or equal to 0.05 were represented. (C) Adour sediments microbial communities modules representation. Visualization of selected modules correlated to trimethoprim and oxolinic acid (C1), to Mn (C2) and to As (C3) illustrating ASVs within each module and their interactions. Each node corresponds to an ASV, node size is proportional to the node betweenness. Modules are identified by colors according to the legend in (A2). For a better resolution version of the Fig., see Fig. S4 for (A1) and (A2) and Fig. S5 for (C1), (C2) and (C3).

Table 1 Contribution of environmental variables on the organization of microbial communities by PERMANOVA based on Bray-Curtis index. Monte Carlo's level of significance (p) below 0.05 are indicated in bold. Only the most significant collinear variables ($coefficient_{pear} \geq |0.85|$) revealed by PERMANOVA are indicated.

Environmental variable	Pseudo-F ratio (F)	R^2	p*	Correlation between variables ($coefficient_{pear}$)
As	4.47	0.061	**0.007**	Vanadium (0.87)
Cr	2.09	0.028	0.065	
Cu	4.25	0.058	**0.001**	
Mn	3.39	0.046	**0.019**	Cobalt (0.90)
Sn	5.91	0.081	**0.001**	
Ti	6.95	0.095	**0.002**	
Zn	4.96	0.068	**0.002**	Losartan (0.85)
Acetaminophen	2.24	0.030	0.052	
Caffeine	2.05	0.028	0.066	
Lorazepam	1.81	0.025	0.126	
Metoprolol	1.57	0.021	0.151	
Norfloxacin	2.57	0.035	**0.048**	
Ofloxacin	2.25	0.031	0.074	
Oxolinic acid	2.61	0.036	**0.043**	Flumequine (0.85)
Trimethoprim	3.77	0.051	**0.011**	
C_{org}/N_{org}	2.91	0.040	**0.028**	
$\delta^{13}C$	4.22	0.058	**0.008**	
Season	2.70	0.073	**0.021**	

*: Monte Carlo approximated level of significance

Figure 1

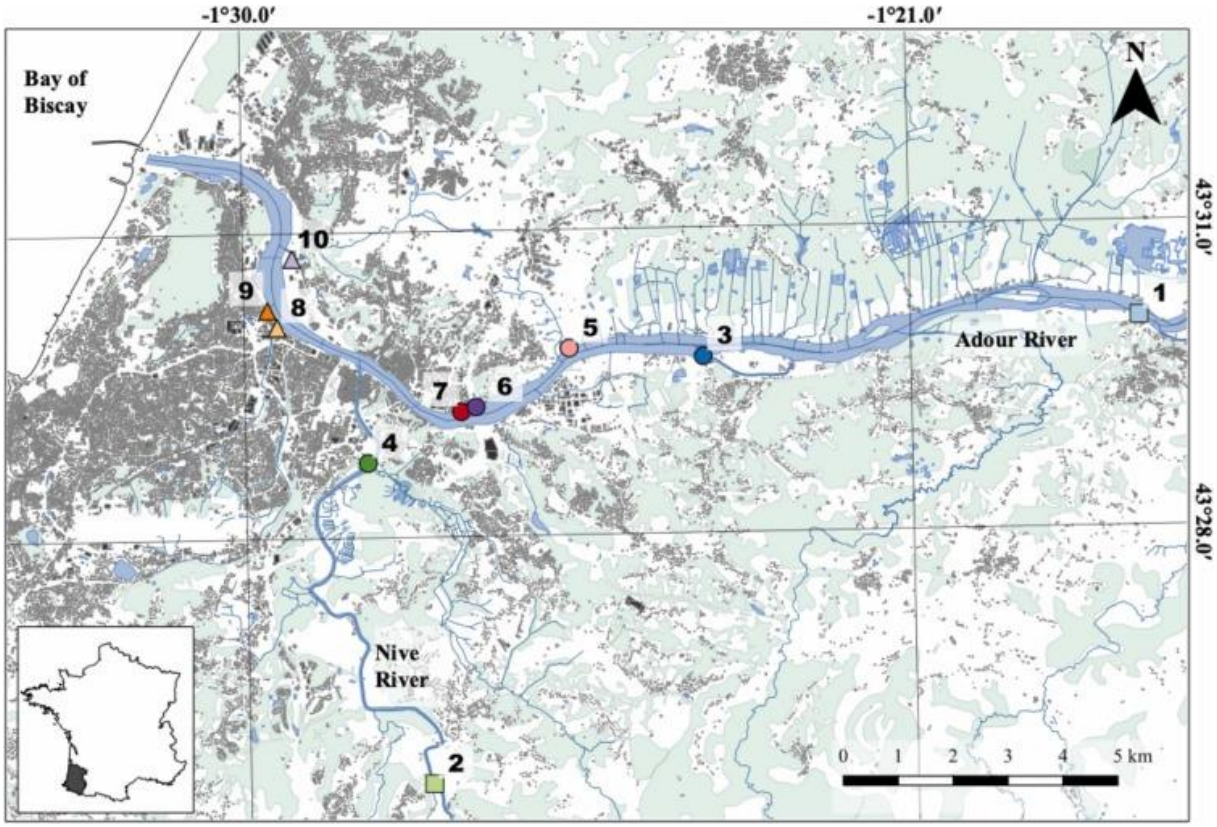

Figure 2

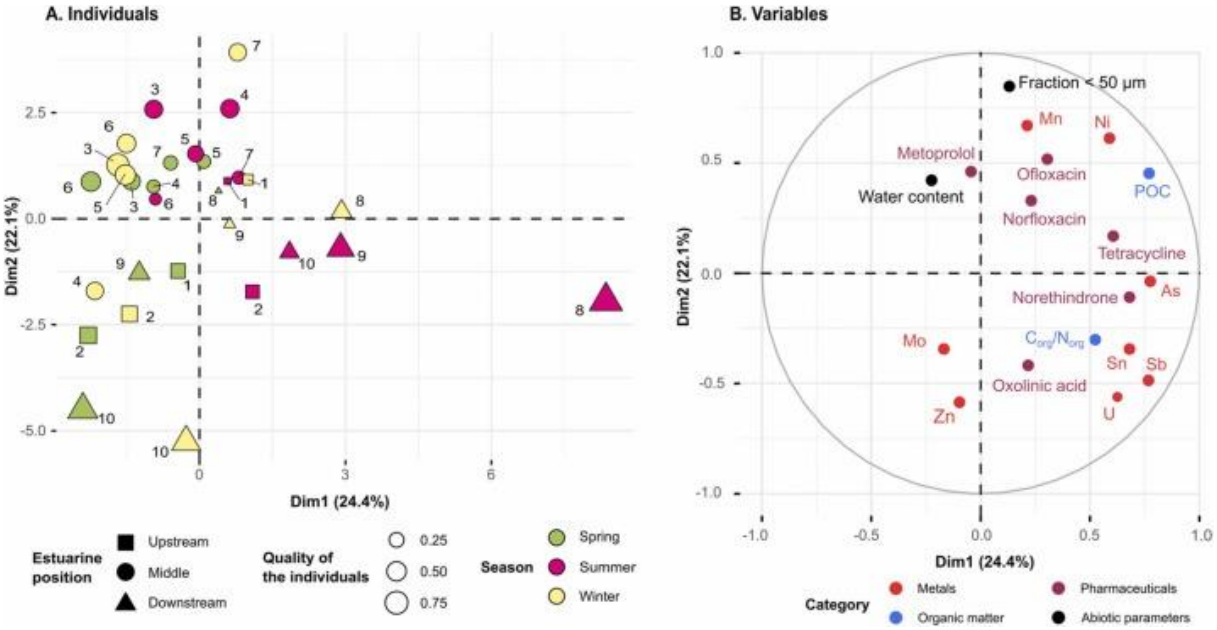

Figure 3

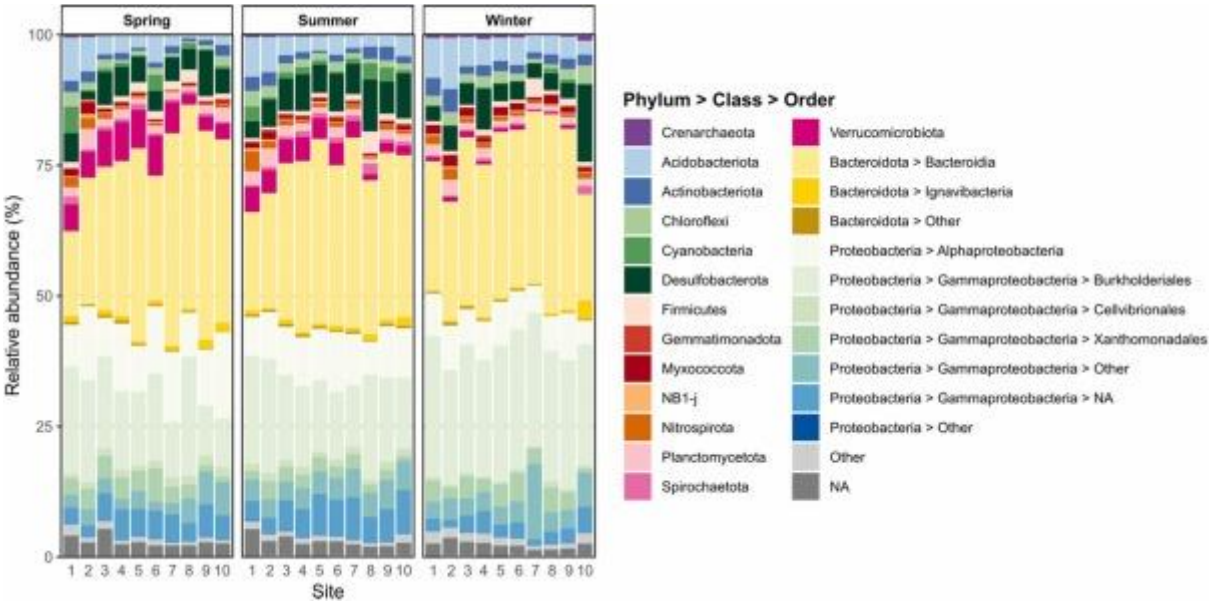

Figure 4

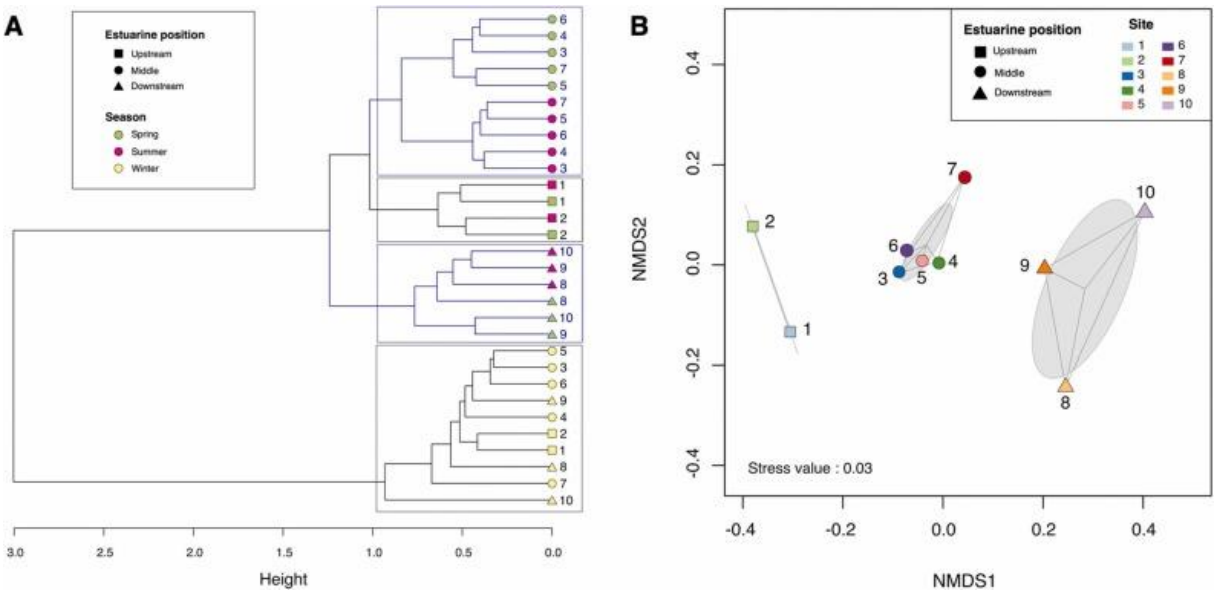

Figure 5

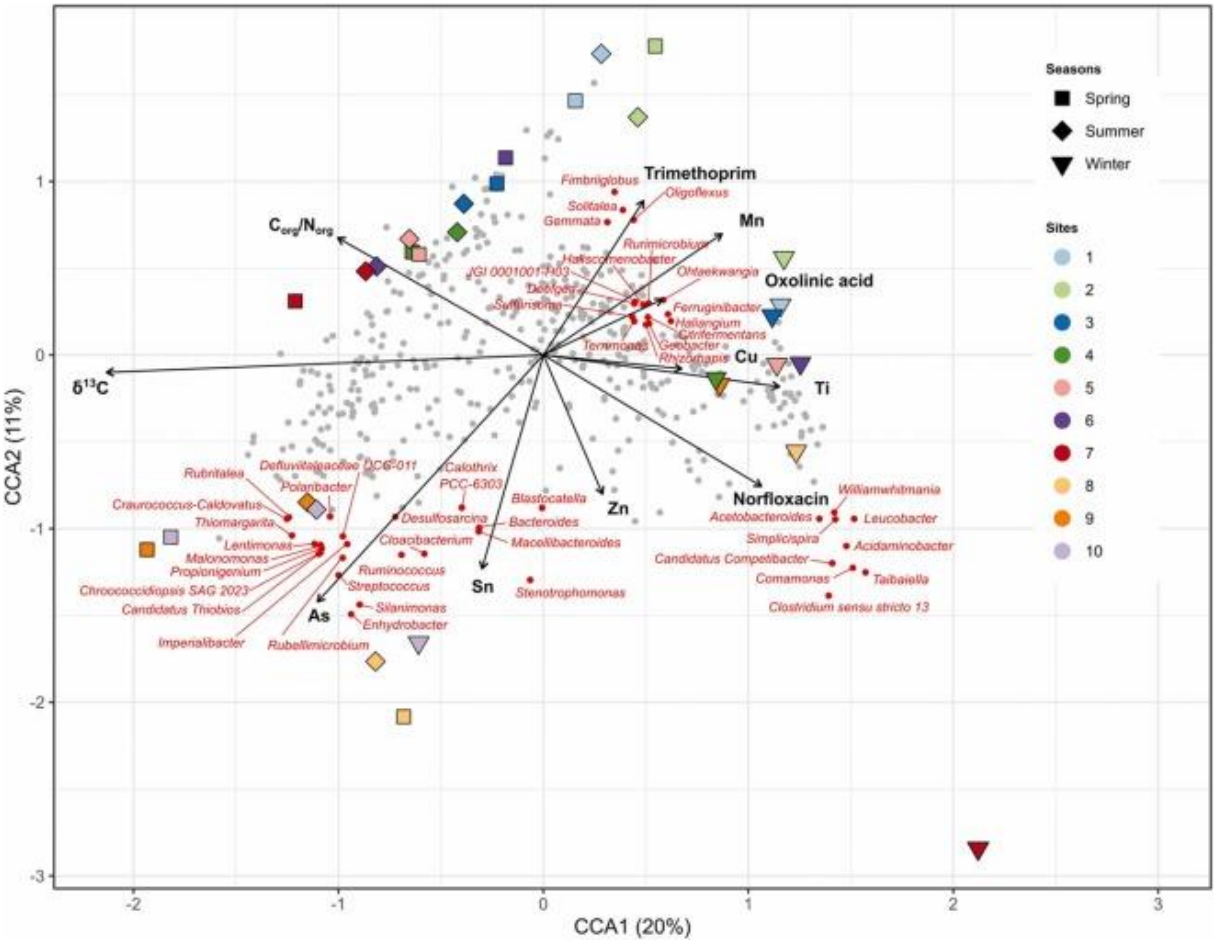
Seasons
Spring
Summer
Winter
Sites
1
2
3
4
5
6
7
8
9
10
Trimethoprim
Mn
Oxolinic acid
Cu
Ti
Zn
Norfloxacin
Sn
As
δ13C
Corg/Norg
Fimbriglobus
Oligoflexus
Solitalea
Gemmata
Runimicrobium
Halioglobus
Ohtaekwangia
Ferruginibacter
Hallangium
Chryseolinea
Rhizomonas
Rubritalea
Defluviitaleaceae DC5-11
Calothrix PCC-6303
Polaribacter
Craurococcus-Caldovatus
Thiomargarita
Desulfosarcina
Blastocatella
Bacteroides
Lentimonas
Cloacibacterium
Macellibacteroides
Malonomonas
Propionigenium
Ruminococcus
Streptococcus
Chroococcidiopsis SAG 2023
Candidatus Thiobios
Silanimonas
Enhydrobacter
Imperialibacter
Rubellimicrobium
Stenotrophomonas
Williamwhitmania
Acetobacteroides
Leucobacter
Simplicispira
Acidaminobacter
Candidatus Competibacter
Comamonas
Taibaiella
Clostridium sensu stricto 13
CCA1 (20%)
CCA2 (11%)

Figure 6

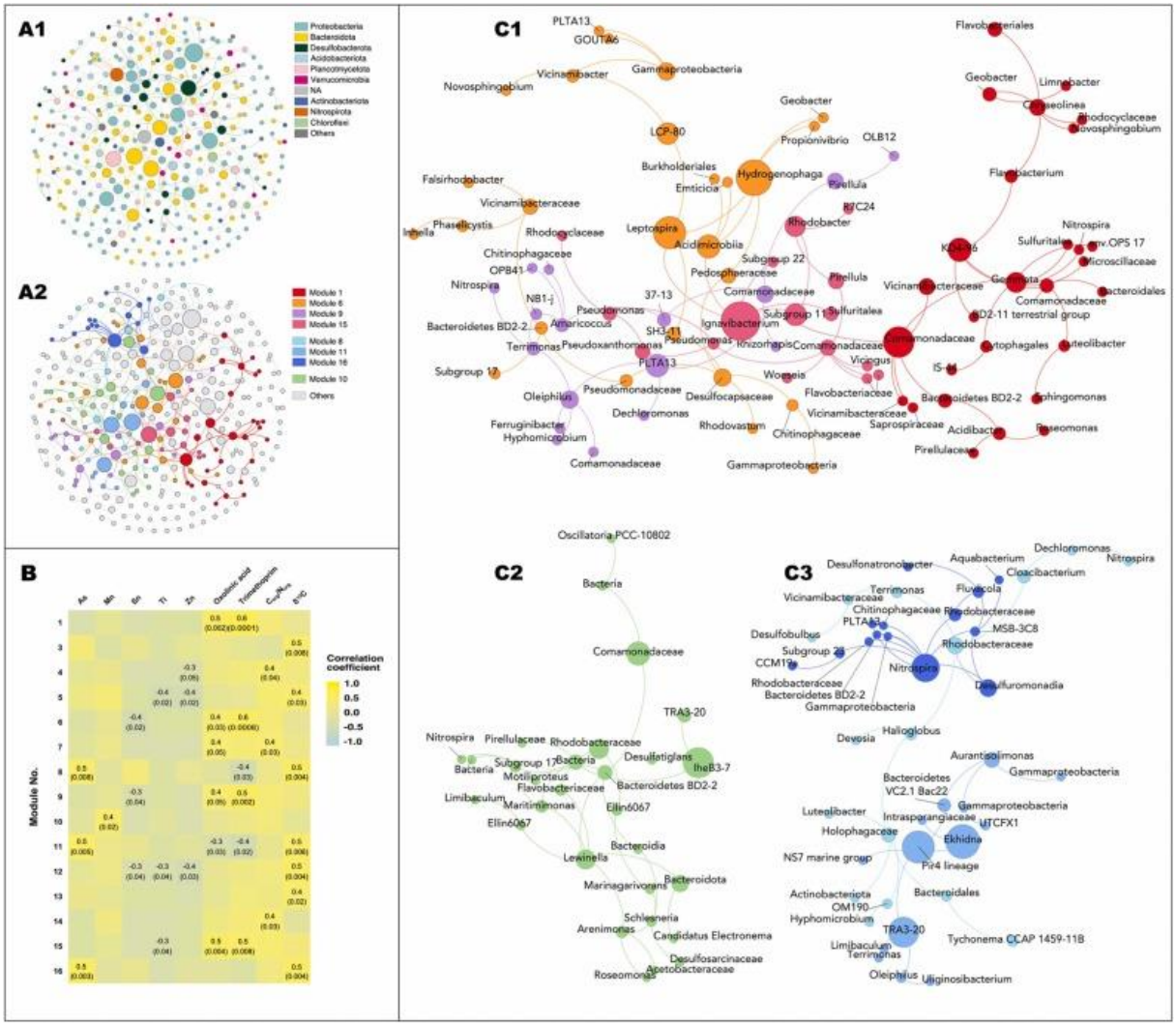
A1
Proteobacteria
Bacteroidota
Desulfobacterota
Acidobacteriota
Planctomycetota
Verrucomicrobia
NA
Actinobacteriota
Nitrospirota
Chloroflexi
Others
A2
Module 1
Module 6
Module 9
Module 15
Module 8
Module 11
Module 16
Module 10
Others
B
As
Mn
Sn
Ti
Zn
Oxalic acid
Trimethoprim
Module No.
Correlation coefficient
1.0
0.5
0.0
-0.5
-1.0
C1
PLTA13
GOUTA6
Vicinamibacter
Gammaproteobacteria
Novosphingobium
Geobacter
LCP-89
Propionivibrio
OLB12
Burkholderiales
Hydrogenophaga
Emticicia
Psellula
Falsirhodobacter
Vicinamibacteraceae
R7C24
Rhodobacter
Phaselicystis
Rhodocyclaceae
Leptospira
Acidimicrobiia
Chitinophagaceae
Subgroup 22
OPB41
Pedosphaeraceae
Pirellula
Nitrospira
Comamonadaceae
NB1-j
37-13
Pseudomonas
Subgroup 11
Sulfuritalea
Bacteroidetes BD2-2
Americoccus
SH3-11
Ignavibacterium
Terrimonas
Pseudoxanthomonas
Rhizorhapis
Comamonadaceae
PLTA13
Subgroup 17
Oleiphilon
Pseudomonadaceae
Desulfocapsaceae
Dechloromonas
Ferruginibacter
Hyphomicrobium
Rhodovastum
Chitinophagaceae
Comamonadaceae
Gammaproteobacteria
Flavobacteriales
Geobacter
Limnobacter
Caldilineae
Rhodocyclaceae
Novosphingobium
Flavobacterium
Nitrospira
Sulfuritalea
env.OPS 17
Microscillaceae
KD4-96
Vicinamibacteraceae
Gemmatimonadota
Bacteroidales
Comamonadaceae
SBR2076
SD2-11 terrestrial group
Gemmatimonadaceae
Cytophagales
Luteolibacter
Vicinus
IS-44
Woeseia
Flavobacteriaceae
Bacteroidetes BD2-2
Sphingomonas
Vicinamibacteraceae
Saprospiraceae
Acidibacter
Roseomonas
Chitinophagaceae
Pirellulaceae
C2
Oscillatoria PCC-10802
Bacteria
Comamonadaceae
TRA3-20
Nitrospira
Pirellulaceae
Rhodobacteraceae
Bacteria
Subgroup 17
Bacteria
Desulfatiglans
IheB3-7
Motiliproteus
Flavobacteriaceae
Bacteroidetes BD2-2
Limibaculum
Maritimimonas
Ellin6067
Ellin6067
Bacteroidia
Lewinella
Bacteroidota
Marinagarivorans
Schlesneria
Arenimonas
Candidatus Electronema
Desulfosarcinaceae
Roseomonas
Apetobacteraceae
C3
Desulfonatronobacter
Aquabacterium
Dechloromonas
Nitrospira
Cloacibacterium
Terrimonas
Fluviicola
Vicinamibacteraceae
Chitinophagaceae
Rhodobacteraceae
PLTA13
MSB-3C8
Desulfobulbus
Rhodobacteraceae
Subgroup 22
CCM19a
Nitrospira
Desulfuromonadia
Rhodobacteraceae
Bacteroidetes BD2-2
Gammaproteobacteria
Devosia
Haloglobus
Aurantisolimonas
Gammaproteobacteria
Bacteroidetes VC2.1 Bac22
Gammaproteobacteria
Luteolibacter
Intrasporangiaceae
UTCFX1
Holophagaceae
Ekhidna
NS7 marine group
Pir4 lineage
Actinobacteriota
Bacteroidales
OM190
Hyphomicrobium
TRA3-20
Tychonema CCAP 1459-11B
Limibaculum
Terrimonas
Oleiphilus
Uliginosibacterium